MODELING OF LNG POOL SPREADING AND VAPORIZATION

A Thesis

by

OMAR MANSOUR ABDELHAFEZ MOHAMED BASHA

Submitted to the Office of Graduate Studies of
Texas A&M University
in partial fulfillment of the requirements for the degree of

MASTER OF SCIENCE

Approved by:

Co-Chairs of Committee,	Sam Mannan
	Luc Véchot
Committee Member,	Eyad Masad
Head of Department,	M. Nazmul Karim

December 2012

Major Subject: Chemical Engineering

ABSTRACT

In this work, a source term model for estimating the rate of spreading and vaporization of LNG on land and sea is introduced. The model takes into account the composition changes of the boiling mixture, the varying thermodynamic properties due to preferential boiling within the mixture and the effect of boiling on conductive heat transfer. The heat, mass and momentum balance equations are derived for continuous and instantaneous spills and mixture thermodynamic effects are incorporated. A parameter sensitivity analysis was conducted to determine the effect of boiling heat transfer regimes, friction, thermal contact/roughness correction parameter and VLE/mixture thermodynamics on the pool spreading behavior. The aim was to provide a better understanding of these governing phenomena and their relative importance throughout the pool lifetime. The spread model was validated against available experimental data for pool spreading on concrete and sea. The model is solved using Matlab for two continuous and instantaneous spill scenarios and is validated against experimental data on cryogenic pool spreading found in literature.

DEDICATION

To my parents

ACKNOWLEDGEMENTS

I am deeply grateful to my advisor, Dr. Luc N. Véchot, for all his feedback and his guidance throughout this process. I would like to acknowledge my committee members: Dr. Sam M. Mannan and Dr. Eyad Masad. Thanks to all the members and staff of the Process Safety Group at Texas A&M University at Qatar. I would like to acknowledge Dr. Simon Waldram for introducing me to the field of process safety and his guidance and help. I want to acknowledge the long term, not only financial, support provided by BP Global Gas SPU for the LNG safety research being conducted at Texas A&M University at Qatar (TAMU at Qatar), and the support of Qatar Petroleum in the form of the facilities used for experiments at RLESC and the provision of staff to work with the TAMU at Qatar's LNG research team.

NOMENCLATURE

A	Pool area (m)
CHF	Critical Heat Flux
C_p	Specific heat Capacity of mixture component (J/kg-K)
C_F	friction coefficient (m/s^2)
g	acceleration due to gravity (m/s^2)
h	pool height (m)
h_s	Heat Transfer Coefficient (W/m^2-K)
k	Thermal Conductivity (W/m-K)
ΔH_{vap}	latent heat of vaporization (J/kg)
Lc	Length Scale (m)
m	LNG mass (kg)
Nu	Nusselt Number (-)
ONB	Onset of Nucleate Boiling
P	Pressure (Pa)
q	Heat flux (W/m^2)
Q	Heat transfer to the pool (W)
R	Universal Gas Constant (J/K-mol)
r	radius (m)
t	time (s)

T	temperature (K)
x	Liquid Mole Fraction (-)
y	Vapor Mole Fraction (-)
z	ground depth (m)
α	Thermal diffusivity (m^2/s)
β	Friction adjustment constsnt (-)
σ	Interfacial tension (N/m^2)
ρ	Density (kg/m^3)
γ	Ratio of liquid inertia at leading edge to that of pool (-)
ν	Viscosity ($kg/s \cdot m$)
χ	Thermal contact/ roughness adjustment parameter (-)
ω	Acentric factor (-)

Subscripts:

a	Ambient temperature
c	Critical temperature
CHF	Critical Heat Flux
cond	Conduction
conv	Convection
i	Component Index
∞	Initial temperature of ground = Temperature of heat sink
j	Component Index

L	Liquid
long	Long wave radiation from the pool
min	Leidenfrost temperature
r	Reduced property
rad	Solar radiation
s	Surface of substrate
Sat	Saturated Pressure
Total	Total Pressure
V	Vapor
vf	Vapor Film
VLE	Vapor Liquid Equilibrium
W	Water

TABLE OF CONTENTS

Page

LIST OF FIGURES

Page

LIST OF TABLES

Page

CHAPTER I

INTRODUCTION

1.1. Background

Liquefied Natural Gas (LNG) is natural gas that has been cooled down to its liquid state at atmospheric pressure. LNG is produced primarily in the Middle East and Russia and is then transported all around the world using tankers and continental pipelines. Over the last few years Qatar has become a key player in the LNG industry. The liquefaction process of natural gas allows a 600 fold reduction in the volume of the gas being transported at ambient pressure. The resulting liquid which is mainly composed of methane presents some hazardous properties linked to its flammable nature and its cryogenic state. Typical composition ranges for LNG and the hazardous properties associated with LNG are shown in Tables 1 and 2 respectively.

Upon a release on land or sea, LNG (boiling point = -162°C) will boil vigorously and generate a vapor cloud that will disperse. If within the flammable range, the vapor cloud may ignite and cause fires and explosions. Although governmental regulations have been imposed and new technologies have been designed and incorporated into the design and operating procedures of LNG facilities, risks associated with catastrophic events like a total loss of containment of an LNG tanker or storage tank must be studied to determine the potential impact on the employees, the facility, the public and the environment.

Table 1: Typical composition of LNG

Chemical	Chemical Formula	Lean	Rich
Methane	CH_4	99%	87%
Ethane	C_2H_6	< 1%	10%
Propane	C_3H_8	> 1%	5 %
Butane	C_4H_{10}	> 1%	> 1%
Nitrogen	N_2	0.1%	1%
Other Hydrocarbons	C_5+	Trace	Trace

Table 2: LNG hazardous properties

Properties	LNG
Toxic	No
Carcinogenic	No
Flammable Vapor	Yes
Forms Vapor Clouds	Yes
Asphyxiant	Yes
Extreme Cold Temperature	Yes
Flash point (°C)	-188
Boiling point (°C)	-160
Flammability Range in Air, %	LEL = 5.5% and UEL 14% (at 25°C)
Auto ignition Temperature ^{0}C	540
Behavior if Spilled	Evaporates, forming a partly visible clouds

Modeling the spread and vaporization of an LNG pool is a key element in the consequence analysis and risk assessment of a possible spill on water or land. This represents an important part of the source term (LNG vapor release rate) which is subsequently used for vapor dispersion modeling. While atmospheric dispersion of flammable vapor has been extensively studied, LNG source term modeling, including pool spreading and vaporization has received less attention both experimentally and theoretically.

In this work, a source term model for estimating the rate of spreading and vaporization of LNG and cryogenic mixtures on unconfined land and sea is proposed. The model takes into account the composition changes of a boiling liquid mixture, the varying thermodynamic properties due to preferential boiling within the mixture and the effect of boiling on conductive heat transfer. A parameter sensitivity analysis was conducted to determine the effect of boiling heat transfer regimes, friction, thermal contact/roughness correction parameter and VLE/mixture thermodynamics on the pool spreading behavior. The aim was to provide a better understanding of these governing phenomena and their relative importance throughout the pool lifetime. The model was validated against available experimental data for pool spreading on concrete and sea.

1.2. Previous accidents involving LNG

Transportation and handling of LNG in import/export facilities has over 60 years of development. Accidents involving LNG often resulted in huge financial and commercial impacts; this section provides a summary of the recorded incidents involving LNG.

1.2.1. Shipping and transportation of LNG

Most of the incidents involving LNG occurred during maritime transport, but there has been insufficient data collection to draw conclusions regarding the safety of LNG maritime transport. Nonetheless, most of these incidents are not specific to LNG itself but are more connected to the practices of the maritime transport industry. Table 3 summarizes shipping accidents that involved LNG from 1995 to 2009. When compared

to oil carriers, LNG tanks seem slightly less incident prone, but when forecasting the expected increase in demand and transportation of LNG over the coming decade, this may very well change. Some of the more significant incidents are highlighted in Table 4.

1.2.2. Land based incidents

Most land based incidents involve a vapor release that was somehow ignited resulting in a wide variety of consequences. These incidents have highlighted the importance of being able to contain LNG vapor from spreading and keeping LNG activities at a safe distance from other plant facilities, particularly combustion, compression and air intake equipment. Moreover, it shows that released LNG vapor on land will probably not travel far before getting ignited. Table 5 highlights the major land based incidents associated with LNG.

Table 3: Accidents involving maritime transport of LNG from 1995 to 2009 (Forsman, 2011)

Cause	**Number of accidents**	**% of Total**	**Killed/ Missing**	**LNG Released (m^3)**
Collision	50	26%	0	7
Contact	8	4%	0	1
Fire/Explosion	26	13%	29	1
Foundered	14	7%	24	2
Hull/ Mchy. Damage	63	32%	0	2
Miscellaneous	1	1%	0	0
Wrecked/ Stranded	33	17%	0	1
Total	195	100%	53	14

Table 4: Major maritime incidents involving LNG

Year	Vessel Name	Status	Consequence	Comment
1969	Polar Alaska	Transportation	LNG Vapor release	Violent sloshing of LNG in refrigerated tank broke the membrane cargo wall resulting in a release of LNG. Spill was not ignited and no fire or explosion was reported.
1971	Descartes	Mechanical Problems	LNG Vapor release	Gas leak from the tank due to a faulty connection between tank dome and membrane wall.
1976	Guayaquil, Ecuador	LNG Unloading	> 50 people injured	A short circuit on the unloading tanker ignited LNG vapor. A series of explosions ensued, destroying five natural gas tanks and wrecked a Shell owned peer for three hours before firefighters were able to contain the fire.
1977	LNG Delta	Loading at terminal	1 killed	Both primary and secondary valves used in the loading station failed upon contact with cryogenic temperatures, resulting in an LNG release but no ignition occurred.
1979	Mostafa Ben Boulaid (Algerian tanker) at Point Cove LNG terminal (US)	LNG Unloading	LNG spill resulting in deck fracture	Check valve failed during unloading, resulting in an LNG release which fractured the deck. The ESD system was activated and water spray systems managed to contain the vapor cloud.

Table 5: Major land based incidents involving LNG

Year	Place	Status	Consequences	Comment
1944	Cleveland, Ohio	Construction failure	128 killed, 225 injured	LNG storage tanks experienced material failures resulting in overflowing of LNG into surrounding dikes. The vapor cloud was ignited. A second tank failed after 20 minutes resulting in more LNG release and a longer fire time. It is estimated that the pool fire extended to 0.5 miles around failed tank.
1966	Raunheim , Germany	Accidental venting	1 killed, 75 injured	LNG was being passed through a vaporizer. The liquid level control loop failed resulting in overflow and around 500 kg of LNG was vented out of the vaporizer. The vapor cloud drifted towards the control room resulting in a fire and explosion.
1968	Portland, US	Human malfunction	4 killed	Natural gas from the inlet lines leaked into an LNG tank through a valve that was supposed to be closed off, but the flange used to close the valve had been removed for the testing leaving the valve slightly opened. Natural Gas accumulated inside the tank got ignited resulting into.
1973	Staten Island, NY,US	Human malfunction	40 killed	An LNG storage tank was emptied, warmed and purged of the combustible gases using nitrogen, and then filled with fresh re-circulating air. This was not done properly and while repairs were being done on the tank, a fire was ignited resulting in the tank roof getting fractured and collapsing. The 40 workers inside died from asphyxiation.
1977	Arzew,	On terminal	1 killed	A terminal worker was frozen to death during loading. A valve rupture sprayed

Table 5 Continued

Year	Place	Status	Consequences	Comment
	Algeria			the worker with LNG.
1978	Das Island, UAE	On terminal	LNG spill	A bottom pipe connection of an LNG tank failed resulting in a spill. It was stopped by closing the internal valve. The resulting vapor cloud dissipated without igniting.
1983	Bontang, Indonesia	Over pressure	3 killed	A blind left in the flare line resulted in the over pressurization of the main liquefaction column which was a vertical shell and tube heat exchanger. The heat exchanger failed and popped and debris was projected as far as 50m killing 3 workers.
1985	Pinson, Alabama	Loading vessel	6 injured	The welding on a patch plate on an aluminum vessel failed during loading. The plate was projectile towards the control room, blowing the windows. The escaping gas was ignited.
1988	Everett, WA, US	On terminal	Vapor release	Operation of LNG transfer was improperly interrupted resulting in a flange gasket to blow and 114 m^3 of LNG were released. The spill was contained and a stable atmosphere prevented the vapor cloud from propagating.
1989	Thurley, UK	Human malfunction	2 workers got burned	Valves were opened for draining out natural gas, but one was left open before operation. LNG was released as a high pressure jet burning 2 workers. The resulting vapor cloud was ignited 30s into the spill covering an area of 40 by 25 m.

Table 5 Continued

Year	Place	Status	Consequences	Comment
1993	Bontang, Indonesia	Leakage to sewer system	Vapor release	During a pipe modification project, LNG leaked into the underground sewer system. LNG underwent rapid vapor expansions that ruptured the pipes.
2004	Skikda, Algeria	Explosion and fire	27 killed, 5 injured	A leak occurred that was pulled into a high pressure steam boiler. The resulting mixture ignited rapidly resulting in an explosive fire and a fireball that damaged surrounding LNG facilities, killing 27 people.

CHAPTER II

BACKGROUND ON POOL SPREADING AND VAPORIZATION

2.1.Introduction

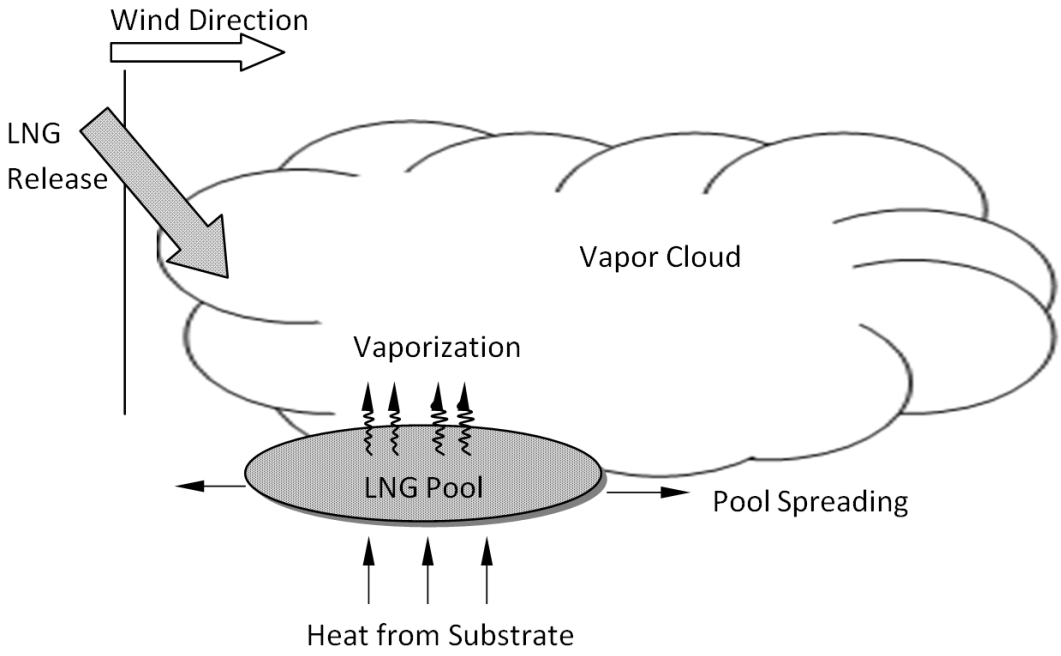

Figure 1: Release dynamics of LNG

Liquid spills can be classified on the basis of the rate, quantity and duration of the spill as follows:

- Instantaneous spill: all of the liquid is spilled at once or over a very short time
- Continuous spill: the spill continues for a significant period of time at a finite rate.

The distinction is made between these scenarios based on a number of factors like the size of the spill, the properties of the spilled liquid and the surrounding environmental conditions. Figure 1 shows the factors involved in the release dynamics of an LNG spill.

Once a release occurs it will usually follow the event tree shown in Figure 2.

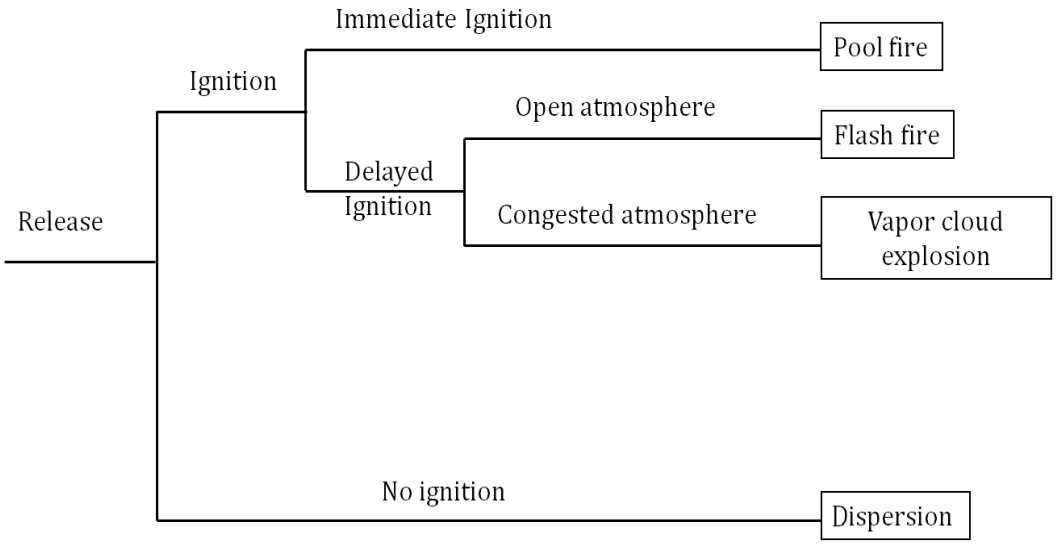

Figure 2: Event tree for an LNG spill

A pool will form from an LNG spill, the behavior of the pool and its dynamics depend on the release scenario and surrounding conditions.

If immediate ignition occurs to the LNG spill a pool fire will develop. This will pose a direct hazard to the surroundings due to direct fire contact and thermal radiation.

In the case where no immediate ignition occurs, the LNG spill will boil-off generating dense gas which is then dispersed by atmospheric turbulence. The cloud will pose flammability and explosion hazards for long distances unless it is diluted below its lower flammability limit. The extent of the vapor cloud hazard depends on the pool spill rate, the pool size and the stability of the surrounding atmosphere.

For LNG spills of significantly long duration, a constant spill rate could results in a steady-state pool when the discharge rate into the pool equals the vaporization rate from the pool.

2.2.LNG pool vaporization

When LNG is spilled onto the ground, heat transfer from the substrate will result in an immediate boil-off. The spill rate, duration of spill, ambient temperature and ground temperature and porosity would determine the LNG boiling regime.

2.2.1. Heat transfer from the ground

According to various literature sources (Webber (1991); Cavanaugh, Siegell, & Steinberg (1994)), conduction from the substrate is the most prevailing mechanism for heat transfer to an LNG pool, whereas the heat gain from other sources such as atmospheric convection or radiation accounts on average for less than 5% of the overall heat transfer to the LNG pool.

2.2.2. Conduction heat transfer

For spills over land, the heat transfer to the pool is generally considered to be transient due to conductive cooling of the substrate.

1-D conduction is usually used when modeling heat conduction from the ground. The model is based on assuming a uniform semi-infinite medium on which the pool spreads; the heat flow rate is given by:

$$Q_{cond} = 2\pi\theta \int_0^{R(t)} \frac{r' dr'}{(t - t')^{0.5}} \tag{1}$$

Where r' is the pool radius at time t' when the new pool segment first comes into contact with fresh ground:

$$\theta = \frac{\chi h_s (T_\infty - T_B)}{(\pi\alpha)^{0.5}} \tag{2}$$

Nonetheless it is important to remember that since the substrate is being cooled by the LNG, a continuous spill would have to eventually reach a maximum evaporation rate, Jensen (1983) shows the following behavior. It is understood that at the latter stages of a spill, the heat transfer from the soil becomes sufficiently low, eventually allowing for heat transfer from the air to become increasingly important. He shows that there is an inverse proportionality between the evaporation rate and the square root of time according to the following correlation:

$$q = \frac{s}{\sqrt{t}} \tag{3}$$

$$s = \left(\frac{\Delta T}{\Delta H_{vap}} \right) \sqrt{\frac{\rho c \lambda}{\pi}} \tag{4}$$

A limitation of the above derivation is that it initially results in infinite evaporation rates. Nonetheless a correction is applied by integrating the area differentials of the above equation:

$$Q_n = dA_1 \frac{8}{\sqrt{ndt}} + dA_2 \frac{8}{\sqrt{(n-1)dt}} + \ldots + dA_n \frac{8}{\sqrt{dt}} \tag{5}$$

To achieve adecaying behavior as shown in Figure 3:

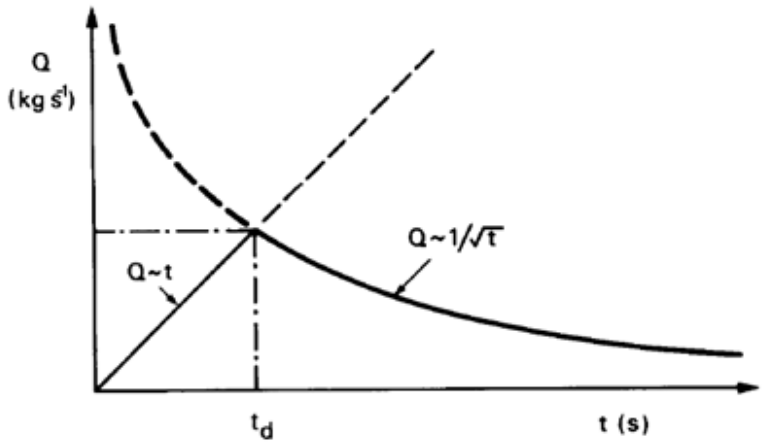

Figure 3: Evaporation rate as a function of time for a continuous release of a cryogenic liquid. (Jensen, 1983)

The point t_d in the above graph corresponds to the time when the pool has reached its maximum area. These results seem reasonable and the conclusion that the evaporation rate would eventually reach a minimum asymptotic value is ok for continuous spills. For

Instantaneous spills it also seems reasonable that a similar, yet steeper profile would exist for the evaporation rate.

2.2.3. Boiling regimes for cryogenic liquids

There are three main pool boiling regimes, as shown in Figure 4, which are functions of the temperature difference between the LNG and the ground, known as the temperature superheat:

1. Nucleate boiling: The LNG is in direct contact with the substrate and bubbles form at distinct intervals.
2. Transitional boiling: There is enough superheat to support vigorous boiling with large distinct bubbles, but not enough to maintain a stable vapor film. At this stage, these large bubbles prevent full thermal contact of the fluid with the surface.
3. Film boiling: There is enough superheat from the substrate to maintain a stable vapor film, thus the LNG is separated from the substrate by a vapor film.

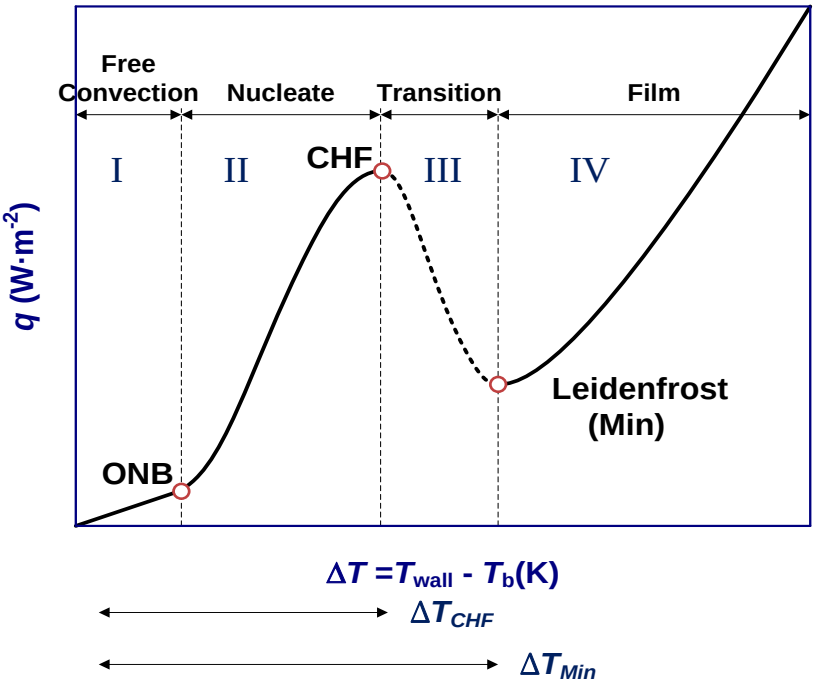

Figure 4: Boiling heat flux curve

When spreading a cryogenic liquid onto the ground, which initially is at ambient temperature, a large temperature difference between the liquid and the ground exists and vigorous boiling will occur. This boiling generates vapor bubbles or a vapor film at the liquid-ground interface which tends to limit the heat transfer. Three boiling regimes can occur depending on the temperature difference between the liquid and the ground: film, transition and nucleate. These complex phenomena make the heat transfer process during boiling difficult to predict.

Experimental measurement of the boiling curve of cryogenic liquids, such as liquid nitrogen (Berenson, 1962) and LNG (Reid & Wang, 1978) are reported in literature. It

has also been reported that LNG will boil in the transitional regime if it has a higher composition of heavier hydrocarbons, if it with a higher content of heavier components tends to boil in the transitional boiling regime (Woodward & Pitblado, 2012). Significant work is still to be done in modeling the boiling of cryogenic liquids. Liu et al. (2011) developed a methodology using Computational Fluid Dynamics (CFD) to simulate the boiling process of liquid nitrogen. This approach is promising and may be extrapolated to calculate the boiling curve for cryogenic liquid mixtures like LNG.

As shown in Figure 4, during the initial stages of the spill when the temperature superheat is relatively high, the pool will be in the film boiling regime and a thin vapor film would be fully developed between the spilled liquid and the substrate over the entire heating surface. The superheat will then start to decrease due to the transient cooling of the ground; until it reaches the minimum superheat ΔT_{min} also known as the Leidenfrost temperature, during this period the heat flux will decrease accordingly until it reaches the minimum value q_{min}. Once the superheat temperature becomes lower than ΔT_{min} the pool will enter into the transitional boiling regime, the transitional boiling regime is usually short lived and involves vigorous boiling and relatively large bubbles due to the breakup of the film, the heat flux will then start to increase due to the increased contact area between the surface and the fluid after the film breakup. The heat flux will increase until it reaches a value of maximum heat flux which corresponds to the critical value q_c, the corresponding temperature is known as the critical superheat and is denoted ΔT_c. As the superheat continues to decrease and drops below the critical superheat, nucleate

boiling will start and the heat flux will continue decreasing with the superheat temperature. During Nucleate boiling, nucleation sites, which are gas or vapor filled cavities, appear on the surface of the substrate and develop to allow vapor bubbles to form. Nucleation can occur on both a solid surface and in a homogenous liquid. The maximum heat flux will occur in the nucleate boiling region, but then decreases sharply as the bubbling becomes so rapid that the liquid is prevented from getting enough contact time with the substrate, this is where the transitional regime starts.

$$\Delta T_{\min} = (T_C - T_L)\left[0.16 + 0.24\left(\frac{\rho_L C_{pL} k_L}{\rho_w C_{pw} k_w}\right)^{1/4}\right] \tag{6}$$

2.2.4. Effect of composition on vaporization rate

Being a mixture of different volatile components, LNG will exhibit preferential boiling. Lighter components will boil off before the heavier ones, resulting in an accumulation of the heavier hydrocarbons within the LNG pool. This change in composition will in turn affect the thermo-physical properties of the LNG pool as it become enriched with the heavier components. It is important to realize that despite methane being the dominant component in LNG, the evaporation rate of an LNG mixture will be different than that of pure methane, particularly during the later stage of boil-off when the methane composition decreases. The vapor liquid equilibrium of a mixture composed of 90 mol% methane and 10% ethane is shown in Figure 5.

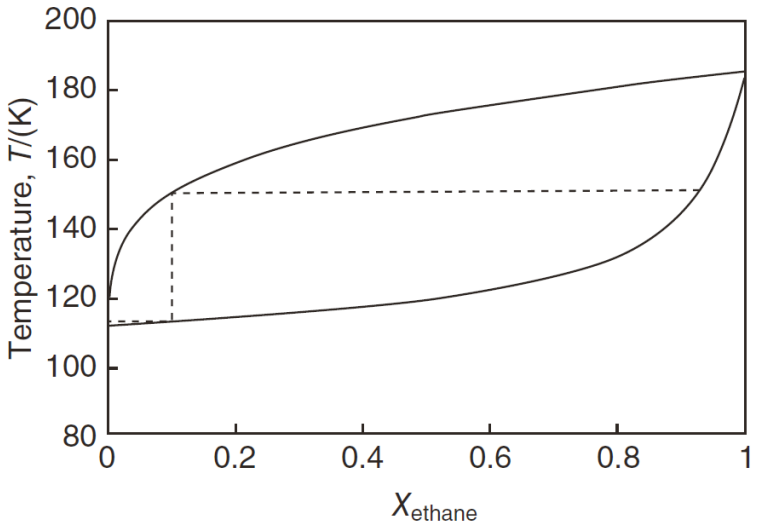

Figure 5: 90 mol% Methane 10mol% Ethane mixture VLE phase envelope

From the above VLE diagram, it is seen that the dew point is very steep for pure methane, while the bubble point is flat. This means that during the initial stages of the spill, the vapor will consist almost completely of methane and the liquid boiling point temperature will change very slowly as exhibited by the flat bubble point curve. Similarly analyzing the other end of the VLE diagram, it is noticeable that the dew point becomes flat whereas the bubble point becomes very steep, this means that during the later stages of the pool life, the vapor composition will not change while the boiling temperature will rapidly increase. These observations have been further verified by plotting the boiling temperature and vapor composition of the mixture over time as shown in Figure 6 (Conrado & Vesovic, 2000):

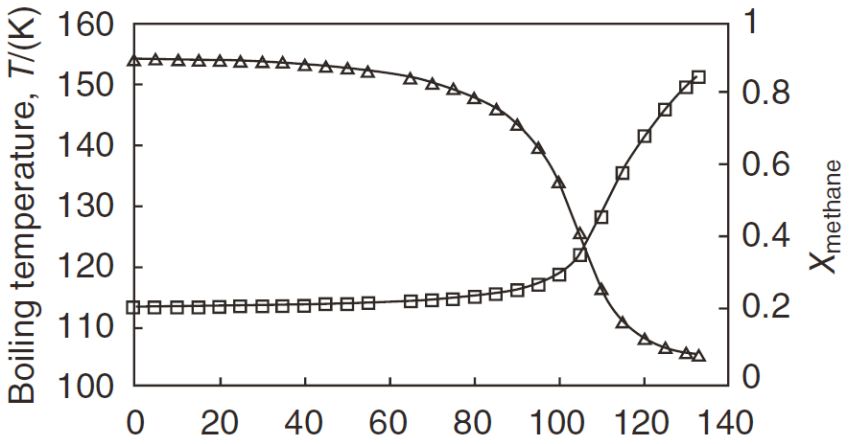

Figure 6: Boiling temperature and vapor composition of 90 mol% methane 10mol% ethane mixture

As predicted, the boiling temperature of the LNG-like mixture remains unchanged during the initial stages and the vaporization rate of the mixture is almost identical to that of pure methane. During the later stages of boiling, and as the LNG becomes increasingly ethane rich, the boiling temperature increases steeply as predicted by the VLE diagram. Therefore as the temperature driving force decreases towards the end of the spill, heat transfer goes from film boiling toe transition boiling stage. This boiling regime is due to the increased content of ethane in the LNG after most of the methane has boiled off during the early stages of the spill. Not considering preferential boil-off would result in underestimating the evaporation time by about 20% (Conrado & Vesovic, 2000). Therefore, when modeling LNG, thermodynamic properties that reflect the behavior of all the compounds in the mixture should be used rather than those of pure methane.

The above conclusions were confirmed by Boe (1998), by performing laboratory scale experiments using liquefied methane-ethane and methane-propane mixtures on boiling water. The results confirmed that the addition of ethane or propane in a predominantly methane mixture will affect the boil off rate in a similar manner to the above. Methane rich mixtures exhibited high initial boil off rates, by adding methane of propane to a 97% methane mixture, the boil off rates increased by a factor of 1.5-2. Moreover, the same conclusion regarding the breakdown of film boiling due to increased contact between the mixture and the substrate which would lead to an enhanced heat flux and lower temperature difference. This ultimately results in the breakdown of the continuous vapor film.

These conclusions were also observed by Drake et al. (1975) which indicated that LNG has a higher boil off rate than pure methane. He conducted a series of laboratory scale experiments with mixtures composed of 98% methane and 2%ethane which is very similar to that of lean LNG. These results were compared to experiments conducted with 82-89% methane mixtures containing ethane-propane ratios between 4-5, which is similar to the composition of rich LNG. His results showed that increasing the amount of heavier hydrocarbons will lead to faster vaporization, and an increased rate of boiling.

2.3.LNG pool spread modeling

As the spilled liquid starts spreading, it will go through several flow regimes due to changes in the dominant forces governing the spread. The forces governing the pool

spreading process are gravity, surface tension, inertia and viscous friction as shown in Figure 7. These different regimes are the basis to many of the models that will be discussed later. There are three main regimes:

1. Gravity-Inertia regime: Gravitational forces are equal to inertial forces.

2. Gravity-viscous regime: Gravitational forces are equal to viscous resistance (More applicable for spills on water)

3. Surface tension regime: Viscous drag forces are equal to the surface tension. (More applicable for spills on land, or spills on water during ice formation)

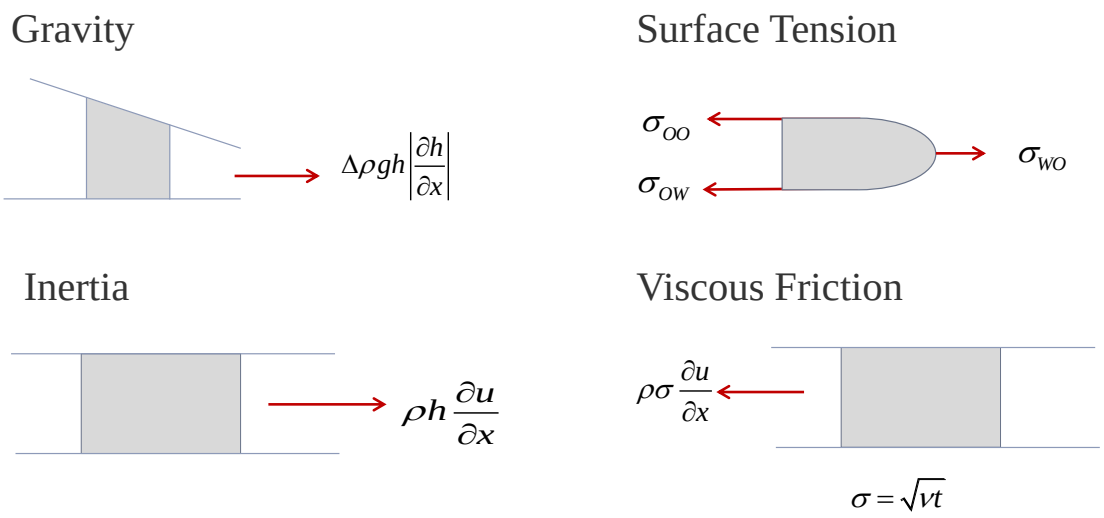

Figure 7: Forces acting on the spreading pool

Each of these regimes could be solved by equating the dominant forces for each regime and obtaining an analytical solution. Since the lifetime of an LNG spill is relatively short, it will spend the entirety of its lifetime in the gravity inertia regime.

CHAPTER III

PREVIOUS EXPERIMENTS ON LNG POOL SPREADING

3.1.Summary of Experiments on liquefied gases

Numerous experiments of various scales have been conducted using LNG, these experiments are necessary to collect a large database of data that can be used to verify models and distinguish among their accuracy and applicability. a comparison of the scale of the most important experiments are shown in Figure 8. Tables 6 to 9 provide a detailed summary of the experiments and the instrumentation used to collect data.

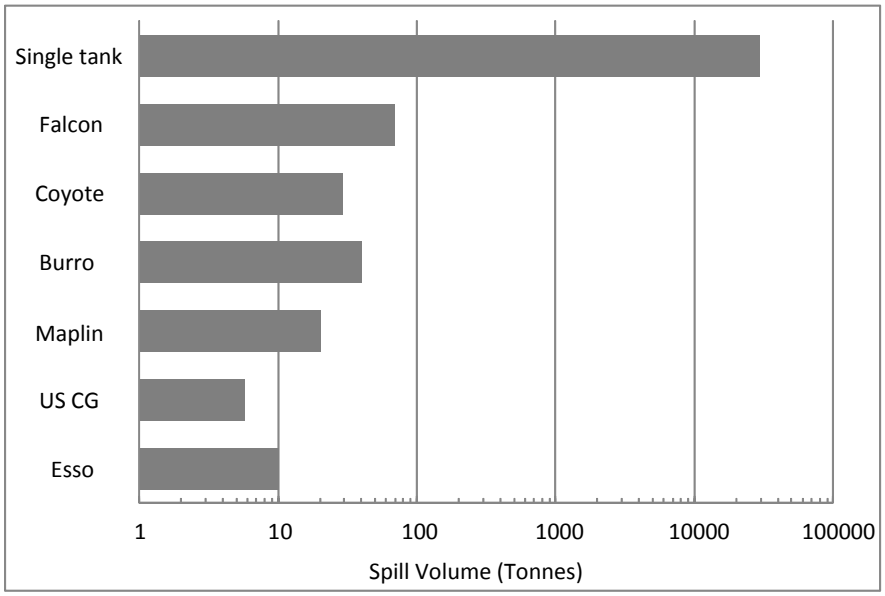

Figure 8: Previous experiments conducted using LNG

Table 6: Spills of liquefied gases into bunds(Puttock, Blackmore, & Colenbrander, 1982)

Experiment	Year	Spilled	Volume (m^3)	Spill Rate (m^3/min)	Duration (min)	No. of tests
Air Products	1966-1967	Oxygen	-	0.04-0.15	30-250	11
AGA/TRW	1968	LNG	0.2	-	0.2	18
Gaz de France	1972	LNG	Max 3	-	-	> 40
Gaz de France	1972	LNG	-	0.16	4.5	1
Battelle/ AGA	1974	LNG	0.4-51	-	0.3-0.5	42 (14 w/ Ignition)

Table 7: Experimental setup for bund experiments

Experiment	Type of Spill	Surface	Bund Size (m^2)	Additional Info	Instrumentation (Sensors)			
					Conc.	Temp	Meteo.	Photo
Air Products	Continuous	Soil	1	Water spray used	6	5	4	-
AGA/TRW	Continuous	- Wet Clay - Dry Clay - Steel	2	-	-	-	3	1
Gaz de France	Instantaneous	Soil	9 – 200	Tipping Bucket	-	-	-	-
Gaz de France	Continuous	Soil	200	-	-	-	-	-
Battelle/ AGA	Instantaneous	- Wet Soil - Dry Soil - Polyurethane	3 – 450	-	36	26	9	-

Table 8: Spills of LNG and other gases onto water (Puttock, Blackmore, & Colenbrander, 1982)

Experiment	Year	Spilled	Volume (m^3)	Spill Rate (m^3/min)	Duration (min)	No. of tests
Bureau of Mines	1970	LNG	0.04-0.5	-	-	51
	1970	LNG	-	0.2-0.3	-	4
	1972	LNG	-	0.2-1.3	Max 10	13 (7 useless)
Esso/API	1971	LNG	0.09-10.2	-	0.1-0.6	17
Shell (Gadila)	1973	LNG	27-198	2.7-19.8	10	6
Shell Maplin Sands	1980	Propane	-	2-5	4-8	11 (3 w/Ignition)
	1980	LNG	-	1-5	1.5-10	13 (4 w/ Ignition)
	1980	Propane	15-25	-	-	3 (1w/Ignition)

Table 8 Continued

Experiment	Year	Spilled	Volume (m^3)	Spill Rate (m^3/min)	Duration (min)	No. of tests
	1980	LNG	5-20	-	-	7 (3 w/ Ignition)
China Lake – Avocet	1978	LNG	4.5	4	-	4
China Lake – Burro	1980	LNG	40	12-18	2.2-3.5	8
China Lake – Coyote	1981	LNG	3-28	6-19	0.2-2.3	5 (w/Ignition) 10 RPT tests
China Lake- Frenchman Flat	1984	Ammonia/ LNG	350	-	-	-

Table 9: Experimental setup of spills on water

Experiment	Type of spill	Surface	Setup	Additional Info.	Instrumentation (Sensors)			
					Conc	Temp	Meteo	Photo
Bureau of Mines	Instantaneous	Water	60 m pond	Tipping Bucket	0	0	1	5
Bureau of Mines	Continuous	Water	60 m pond	-	12	0	1	5
Bureau of Mines	Continuous	Water	70 m lake with 20 m walls	-	30	0	1	1
Esso/API	Instantaneous	Sea	From Barge	Jet 7 m high, 30^0 upwards	18	2	9	2
Shell 'Gadila'	Continuous	Sea	From Ship	Jet 18 m high, Moving ship	0	0	2	3
Shell Maplin Sands	Continuous	Water	300 m pond	3 m above	200	70	45	7

Table 9 Continued

Experiment	Type of spill	Surface	Setup	Additional Info.	Instrumentation (Sensors)			
					Conc	Temp	Meteo	Photo
Shell Maplin Sands	Instantaneous	Water	surrounded by sand	surface				
Shell Maplin Sands	Instantaneous	Water		Sinking Barge				
Shell Maplin Sands	Instantaneous	Water						
China Lake – Avocet	Continuous	Water	Irregular surface for 25 m downwind of source, them 7 m elevation over 80 m from source.	Jet Submerged 1 m into splash plate	11	24	17	1
China Lake – Burro	Continuous	Water			90	100	76	4
China Lake – Coyote	Continuous	Water						
China Lake-Frenchman Flat	Continuous	Water						

CHAPTER IV

CURRENT STATE OF THE ART

4.1.Introduction

In the scenario of a spill of a cryogenic liquid on land, the following parameters will determine the behavior of the pool spread:

1. The type and volume of the release, i.e. instantaneous or continuous;
2. The volatility of the spilled material and its initial temperature (degree of sub-cooling).
3. The thermal (temperature, thermal diffusivity, thermal conductivity) and mechanical (roughness, porosity) properties of the substrate;
4. The presence of any bunds or wall to contain the spill.

A multitude of pool spread models have been developed since the early 70's, although most of them employ the same principles derived for oil spill applications; many have been adjusted to account for LNG applications. The following section will discuss some of the more widely used models.

4.2.Early spread models

Earlier models by Hoult (1972) and Fay (1971) were generally derived from the steady-state Bernoulli equation assuming axisymmetric spread on water:

$$\frac{dr}{dt} = \sqrt{gh} \tag{7}$$

These models assume that gravity is the only driving force for pool spread, while ignoring the effect of friction and preferential boil. It is derived from the balance of the liquid inertia and gravitational force assuming the ground is smooth. Although these models may seem reasonable for oil spills or other heavy liquids, they cannot be applied to cryogenic liquids where the effect of gravity decreases with time. Moreover, the pool radius is dependent on another unknown variable which is the average height of the pool.

These models, although used to represent the gravity inertia regime, do not represent a pure gravity-inertia regime but rather the gravity-front resistance.

Another early model developed by Raj (1974) was derived by equating the inertial resistance forces to gravitational forces as follows:

Inertial resistance:

$$F_l = -C(\pi r^2 h \rho)\frac{d^2 r}{dt^2} \tag{8}$$

Gravitational forces:

$$F_G = \pi r h^2 \rho g \tag{9}$$

Nonetheless this will yield a similar result to the previously mentioned models by reaching the conclusion that spreading is strictly gravity driven

$$\frac{d^2 r}{dt^2} = \frac{gh}{Cr\rho} \tag{10}$$

A setback of these modesl involves the improper repersentation of the gravity inertiea regime, by including a negative sign for the inertial resistance equation, this resulted in a widely used misconception that has been propagated throughout later models (Webber, 1996). Moreover, a basic counterargument against these approaches has also been that they ignore frictional resistance to spreading. These issues were addressed by Webber (1991) who expressed inertial forces as the differences between the gravitational drive and the resistance as follows:

$$\frac{d^2 r}{dt^2} = \frac{4gh}{r} - C_F \tag{11}$$

This effect of gravity was then examined by ABSG & FERC (2004) by comparing theBriscoe & Shaw (1980) model which ignores the effect of friction to that of Webber (1991) mentioned above. Reaching the conlusion that frictional effects are much more significant for large short duration spills, but their effect declines for longer duration spills.

4.3.PHAST

PHAST is a commonly used consequence analysis code, it was developed by DNV and includes models for spill discharge, pool formation, pool evaporation, buoyant and dense gas dispersion, jet fires, pool fires, BLEVE's and vapor cloud explosions.

The integral model used by PHAST for pool spreading and vaporization takes the following effects into consideration:

- Spread on land or water
- Instantaneous or continuous release
- Interaction with bund walls
- Heat conduction from substrate
- Ambient convection for atmosphere
- Radiation and diffusion effects

PHAST adopts the following equation to model for spreading on land:

$$\frac{dr}{dt} = \sqrt{2g(h - h_{\min})} \tag{12}$$

The model assumes that once the pool reaches its minimum height ($h = h_{min}$) , the radius becomes constant as $dr/dt = 0$, ignoring the shrinking effects on the pool induced by evaporation, additionally frictional effects are ignored.

4.4.Supercritical pool spread model

Fay (2007) claimed that the above gravity inertia based models are not entirely applicable to cryogenics due to their unique thermo-physical properties, the proposed model is based on the idea that the vigorous boiling of LNG means that bubbles will occupy a significant volume of the overall pool volume, therefore reducing the density. This reduction in density will both affect the amount of LNG submerged in water for water based spills, and increase the predicted diameter for land based spills. Moreover, this supercritical model argues that equating viscous and gravitational effects as done by Webber might not necessarily be applicable to LNG as it will eventually ride on a thin film of LNG vapor that is at a much lower viscosity than that of water, which then enables the treatment of the LNG pool as inviscid flow. According to the model the pool volume changes are modeled as follows:

$$\frac{dV_p}{dt} = \frac{G_{evap}}{\rho_L}(\pi R^2) = \frac{G_{evap}}{\rho_L}(\pi u_L^2 t^2) \tag{13}$$

The above relation has been derived through an energy balance equation the pool's kinetic energy to the initial potential energy; it argues that gravitational effects should not be a parameter for a continuous release since it is overcome by the initial potential energy of the release. The major disadvantage of this model is that it tries to account for the mechanical effects of boiling by incorporating bubble volume, but fails to account for their heat effects as the vaporization rate is fixed. Moreover, although it accounts for density changes due to bubble volumes, the model does not also incorporate similar changes due to preferential boiling.

4.5.CFD models

CFD codes have yet to achieve full confidence in dealing with LNG release and dispersion modeling. So far only one CFD tool (FLACS) has passed the MEP (model evaluation protocol) for the NFPA-59A standard, whereas countries like France and the Netherlands have moved away from using CFD for Risk assessment of atmospheric dispersion. At the moment, CFD modeling is highly dependent on the user, and different users modeling the same scenario could possibly end with varying results. Moreover, although CFD could arguably provide a better mathematical accuracy, the computational time required compared to integral models is disparaging.

4.5.1. FLACS by GexCon

The FLACS source term model is based on the shallow layer equations presented by Hansen et al. (2007), despite recent enhancements to their code, they still rely heavily on shallow water modeling to predict their pool size and evaporation rate. The 2-D shallow layer model implemented by FLACS relies on the following coupled momentum and heat equations:

$$\frac{\partial u_i}{\partial t} + u_j \frac{\partial u_i}{\partial x_j} = F_{g,i} + F_{\tau,i} \tag{14}$$

$$\frac{\partial \theta}{\partial t} + u_i \frac{\partial \theta}{\partial x_i} = \frac{\dot{m}_L}{\rho_l}(\theta_L - \theta) + \dot{q}_c + \dot{q}_{rad} + \dot{q}_g + \dot{q}_{evap} \tag{15}$$

For spills on water, the conduction heat effects used by FLACS attempt to take into account the effect of the transition and boiling regimes, it uses the correlations derived by Conrado & Vesovic (2000). Moreover, it takes into account the effect of turbulent mixing that is expected to accompany LNG spills on sea as derived by Hissong (2007), who introduces a turbulence factor to model the instability of the thin film during film boiling and the increased contact between the LNG and water due to excessive turbulence disturbing the separating thin film.

The above equations are then solved explicitly using a 3^{rd} order Runge-Kutta solver to obtain the evaporation and geometrical parameters for the spill.

Despite being tested for liquid hydrogen spills as shown by FLACS literature, this shallow layer model has yet to be verified for LNG. Moreover, FLACS will model LNG using an analogue with fixed thermo physical properties, thus ignoring preferential boil off and property changes of the spilled LNG throughout the pool lifetime.

CHAPTER V

METHODOLOGY

5.1.Introduction

In this work, a model is developed that accounts for both the mixture and cryogenic natures of LNG. The model takes into account the composition changes of a boiling mixture due to preferential boil-off and the effect of different boiling modes on conductive heat transfer. The heat, mass and momentum balance equations are derived for different spill scenarios and the model is solved using Matlab.

Unlike currently available models, the uniqueness of this model lies in its incorporation of these complexities to determine the pool behavior and vaporization rate throughout the spill lifetime. Additionally, a purely analytical approach is implemented without relying on any empirical constants or adjustments.

As a mixture, LNG will experience preferential boil-off, which in turn will influence the mixture density, temperature (and therefore heat transfer driving force), viscosity and almost all of the remaining properties as it is continuously changing in composition. Moreover, being a boiling liquid, both the mechanical and heat effects will differ depending on the boiling regime it is currently in. Once these complexities are understood and accounted for, they can then be applied to a wide variety of scenarios and conditions.

5.2.Governing equations

A box model approach has been used to model the spill behavior, the basic idea of the model is shown in Figures 9 and 10. In this model a circular pool with average height is used to predict the behavior of the spill and the height and radius are recalculated for each time step after solving the momentum and heat balance equations.

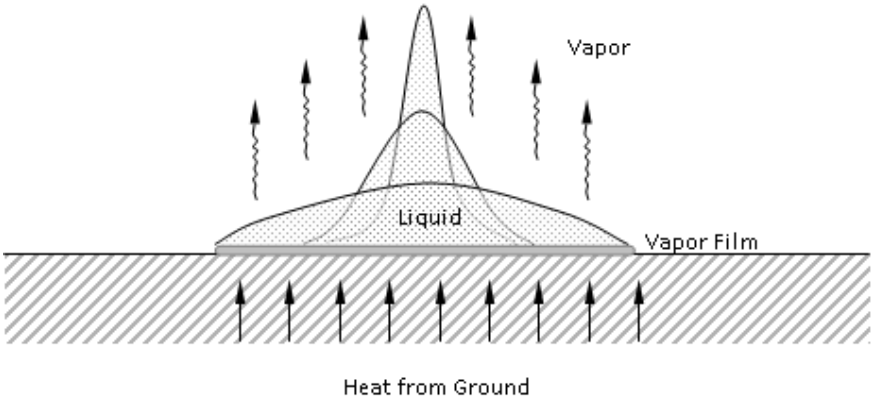

Figure 9: Cryogenic spread on land

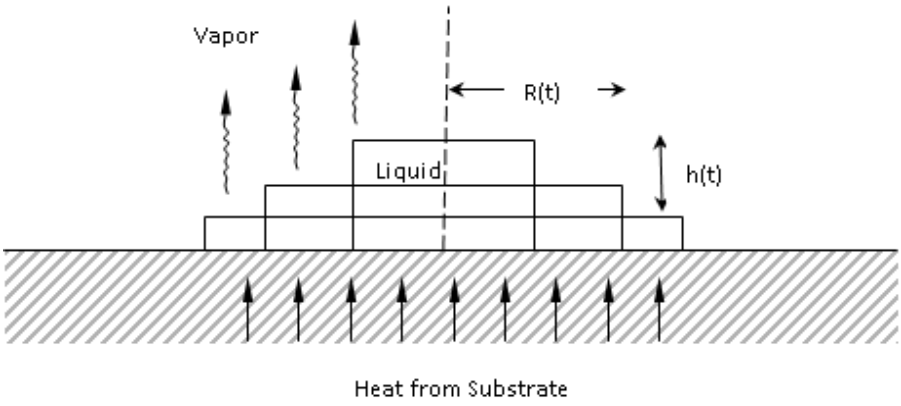

Figure 10: Box model

5.2.1. Mass balance

The volume of the pool is calculated using a mass balance that accounts for the added LNG from the source and the vaporized LNG form the pool at each time step.

$$V = V_0 + \dot{V}_c t - \frac{m_{vap}}{\rho} \tag{16}$$

The average height of the liquid pool is then calculated by:

$$h_{pool} = \frac{V}{\pi r^2} \tag{17}$$

5.2.2. Momentum balance

The momentum balance is based on a gravity-inertia regime, with the addition of a resistance term corresponding to the friction at the base of the pool:

$$Inertial\ forces\ =\ Gravitational\ forces\ -\ Friction \tag{18}$$

The equation describing the spreading rate of the pool is then given by (Webber , 1991):

$$\frac{\partial^2 r}{\partial t^2} = \frac{1}{\gamma} g \frac{h}{r} - C_F \tag{19}$$

The adjustment constant γ is a multiplicative constant derived from the self-similar solutions of the shallow layer equations for a radial spread of a fixed volume of liquid as shown by Webber (2012). Other models account for this multiplicative difference by deriving the ratio of the liquid inertia of the leading edge to that of the pool bulk (Briscoe & Shaw (1980)). A value of 0.25 is used for γ as shown by Webber et al

(1987). The frictional resistance terms were calculated using the correlations provided by Webber (1991).

5.2.3. Heat transfer to the pool and boiling regimes

Equation (19) is coupled to the following equation describing the vaporization rate:

$$\frac{dm}{dt} = \frac{Q}{\Delta H_{vap}} \tag{20}$$

The heat flux into the pool will be determined by the boiling regime, the behavior of the boiling pool will follow the trend shown in Figure 4. The maximum heat flux and critical temperature for nucleate boiling can be estimated using the following equation (Conrado & Vesovic (2000)):

$$q_{\max} = q_{cr} = 0.16\Delta H_{VL}\rho_V^{1/2}[\sigma g(\rho_L - \rho_V)]^{1/4} \tag{21}$$

$$\Delta T_{cr} = 0.625(q_{cr}\sigma T_L)^{1/3} \frac{\left[\frac{10}{(\rho_w C_{pw} k_w)^{1/2}} + (\sqrt{v/k_L})\right]^{2/3}\left[1+10\left(\frac{\rho_L C_{pL} k_L}{\rho_w C_{pw} k_w}\right)^{1/2}\right]^{1/3}}{1+10\left(\frac{\rho_{vs}}{\rho_L - \rho_{vs}}\right)^{2/3}} \tag{22}$$

The minimum heat flux and temperature indicating the transition to film boiling regime can also be estimated using the following equation (Kalininet al., 1976; Opschoor, 1980):

$$q_{\min} = 0.18 k_v \Delta T_{\min} \left[\frac{g}{\nu_v \alpha_v} \left(\frac{\rho_L}{\rho_v} - 1 \right) \right]^{1/3} \tag{23}$$

Figure 11 shows the boiling heat flux curves for the LNG components. LNG is expected to lie somewhere between methane and ethane. No correlations have been developed for mixtures.

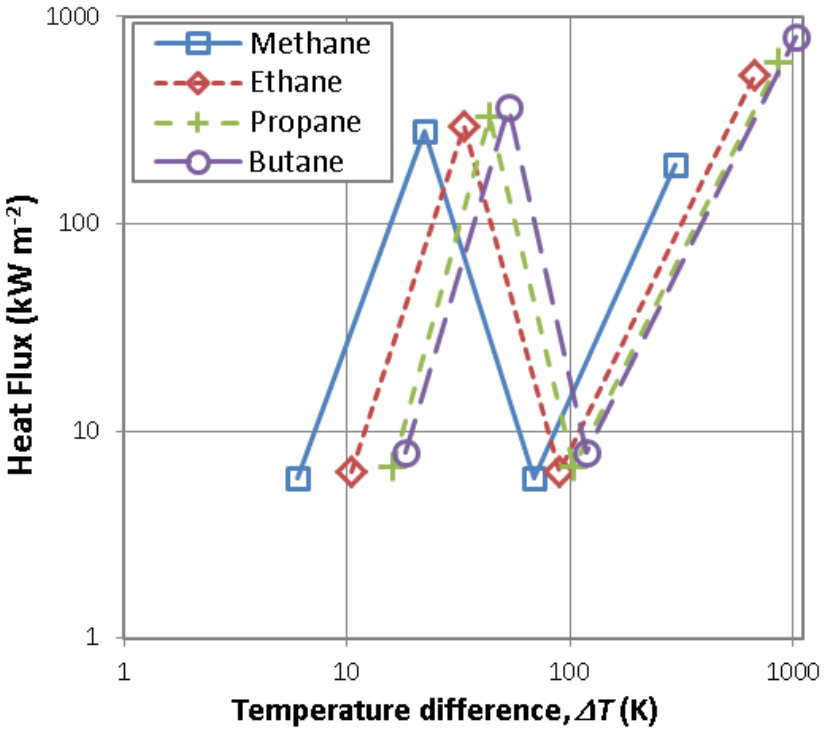

Figure 11: Boiling heat flux curves for LNG components

The correlation provided by Klimenko (1981) was used to determine the heat flux into the pool during the film boiling:

$$q_{cond\_film} = h_{S\_film} \left(T_a - T_L \right) \tag{24}$$

The heat transfer coefficient for film boiling is expressed as a function of the Nusselt number, thermal conductivity of the vapor film and a characteristic length as follows:

$$h_{S\_film} = \frac{Nu_S k_{Vf}}{L_C} \tag{25}$$

The Length scale factor:

$$L_C = 2\pi\sqrt{\frac{\sigma}{g(\rho_L - \rho_V)}} \tag{26}$$

The criteria to determine Laminar or Turbulent flow in the vicinity of the vapor film is as follows:

$$\text{Laminar Region}: \quad Ar < 10^8, \quad Nu_S = 0.19(Ar\,\text{Pr})^{1/3} f_1 \tag{27}$$

$$\text{Turbulent Region}: \quad Ar < 10^8, \quad Nu_S = 0.19(Ar\,\text{Pr})^{1/3} f_1 \tag{28}$$

Where:

$$Ar = (2\pi)^3 \frac{\sigma^{1.5}\rho_V}{\mu_V^2\sqrt{g(\rho_L - \rho_V)}} \tag{29}$$

$$\text{Pr} = \frac{C_{PV}\mu_V}{k_V} \tag{30}$$

Where f_1 and f_2 are functions of the thermal properties of the liquid pool, determined as follows:

$$\text{Laminar Region}: \quad \begin{cases} 1 & for \quad \left(\frac{\Delta H_{LV}}{C_{pL}\Delta T}\right) \le 1.4 \\ 0.89\left(\frac{\Delta H_{LV}}{C_{pL}\Delta T}\right)^{1/3} & for \quad \left(\frac{\Delta H_{LV}}{C_{pL}\Delta T}\right) > 1.4 \end{cases} \tag{31}$$

$$\text{Turbulent Region}: \quad \begin{cases} 1 & for \quad \left(\frac{\Delta H_{LV}}{C_{pL}\Delta T}\right) \le 2 \\ 0.71\left(\frac{\Delta H_{LV}}{C_{pL}\Delta T}\right)^{1/2} & for \quad \left(\frac{\Delta H_{LV}}{C_{pL}\Delta T}\right) > 2 \end{cases} \tag{32}$$

The correlation provided by Opschoor (1975) was used to calculate the heat transfer for the nucleate regime, whereas the heat flux for the transitional regime is determined using a linear approximation between q_{CHF} and q_{Min}.

The change from transition to nucleate boiling happens at the critical superheat corresponding to the ΔT_{CHF} point on Figure 4. Kalinin et al. (1976) proposed the following correlation:

$$\Delta T_{CHF} = 0.625(q_{CHF}\sigma T_L)^{1/3} \frac{\left[\frac{10}{(\rho_w C_{pw} k_w)^{1/2}} + (\sqrt{\upsilon / k_L})\right]^{2/3}\left[1+10\left(\frac{\rho_L C_{pL} k_L}{\rho_w C_{pw} k_w}\right)^{1/2}\right]^{1/3}}{1+10\left(\frac{\rho_{v,s}}{\rho_L - \rho_{v,s}}\right)^{2/3}} \tag{33}$$

The condition for nucleate boiling to occur is:

$$\Delta T < \Delta T_{CHF} \tag{34}$$

A similar condition is applied to determine whether transition boiling occurs by determining the minimum temperature required for film boiling. This is calculated using the correlation from Kalinin et al. (1976):

$$\Delta T_{Min} = (T_C - T_L)\left[0.16 + 0.24\left(\frac{\rho_L C_{pL} k_L}{\rho_w C_{pw} k_w}\right)^{1/4}\right] \tag{35}$$

The condition for transition boiling to occur is:

$$\Delta T < \Delta T_{Min} \tag{36}$$

Else film boiling is present. The algorithm used to implement boiling heat transfer is shown in Figure 12.

Unlike 1-D conduction, the Drichlet boundary condition used to determine the ground temperature is not valid when boiling is considered, as the thermal resistance between the ground surface and the liquid pool should be accounted for. A Neumann type boundary condition was therefore applied to calculate the ground surface temperature. An in-house model was developed under Matlab to account for the change of surface temperature based on the heat transfer correlations for the boiling regimes cited above.

$$T_0^{t+\Delta t} = T_0^t + n\left(T_{\Delta x}^t - T_0^t + \frac{\Delta x}{k} q^t\right) \tag{37}$$

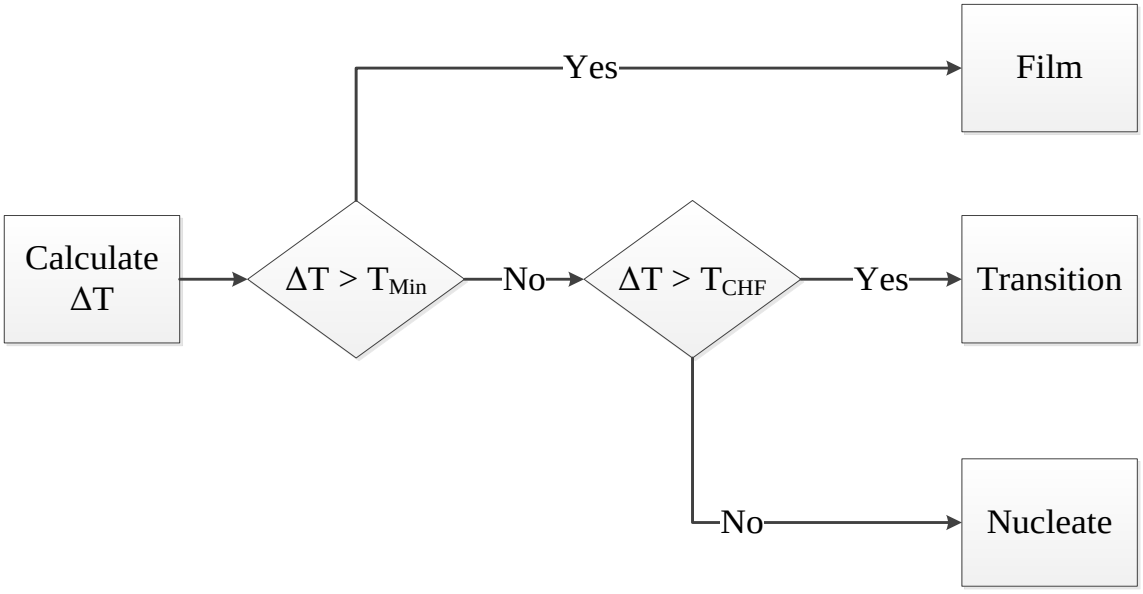

Figure 12: Algorithm for Heat transfer as implemented in the proposed model

5.2.4. LNG pool/ vapor properties – vapor liquid equilibrium

The use of pure fluids or constant property analogues to represent LNG may not provide an accurate representation of its mixture thermodynamics (Conrado & Vesovic, 2000). Varying the thermo physical properties and composition throughout the pool spread period have to be accounted for. LNG will behave differently than pure methane, or in fact a pure cryogen, as transient changes in the composition may affect the physical properties of the mixture. Vapor Liquid Equilibrium (VLE) relations can be used to predict such properties and were incorporated in the pool spreading model as follows.

Since the system will always be at low pressure, Raoult's law was used to calculate the partial pressure of each component in the vapor phase.

$$x_i P_{i,sat} = y_i P_{total} \tag{38}$$

The saturation properties for each of the pure components were calculated using the Antoine Equation.

$$\log_{10} P = A - \frac{B}{C + T} \tag{39}$$

Where A, B and C are component specific empirical constants.

The enthalpy of vaporization was determined as the difference between the vapor and liquid enthalpies:

$$\Delta H_{Vap} = H_V - H_L \tag{40}$$

The enthalpy of each of the phases is calculated as the sum of the ideal gas and residual enthalpies:

$$H_{phase} = H^{ig}_{phase} + H^{residual}_{phase} \tag{41}$$

For the gas phase, the ideal gas enthalpy was determined using the following mixing law:

$$H^{ig}_V = \sum_i x_i \left(\int_{T_0}^{Tsat} C^{ig}_{P,i} dT + H^{ref\,(T,P)}_{formation,i} \right) \tag{42}$$

The reference state was taken to be at 298 K and 1 atm.

The ideal gas heat capacity of each of the components was determined using the Shomate equation:

$$C_{Pi} = A + B \cdot T + C \cdot T^2 + D \cdot T^3 + \frac{E}{T^2} \tag{43}$$

Where A, B, C, D and E are empirical constants obtained from the NIST Database.

The residual enthalpy of the vapor phase was ignored because the system will be at low pressure.

The enthalpy of the liquid phase was determined similar to Equation 23, an ideal solution mixing rule was used and the mixing energy was neglected as follows:

$$H_L = H_L^{ig} + H_L^{res} = \sum_i x_i H_{L,i} + H_L^{mix} = \sum_i x_i H_{L,i} \tag{44}$$

The pure component liquid enthalpy was then determined as follows:

$$H_{L,i} = H_i^{ig} + H_i^{res} = \int_{T_0}^{Tsat} C_{P,i}^{ig} dT - \Delta H_i^{vap} \tag{45}$$

The pure component residual enthalpy was taken to be equal to the negation of the vaporization energy, because the saturated vapor is assumed to behave as an ideal gas at the temperature of interest.

The heat of vaporization of the pure components was determined using the Pitzer correlation:

$$\Delta H_i^{vap} = RT_{c,i}(7.08(1-T_{r,i})^{0.354} + 10.95(1-T_{r,i})^{0.456}\omega_i \tag{46}$$

The heat of vaporization of the mixture is then calculated using Equation 40 and used to determine the vaporization rate from the spreading pool.

The algorithm used to implement mixture thermodynamics is shown in Figure 13.

5.2.5. Differences between pool spread on land and water

In this work, the major difference between the pool spread models on land and on sea involved accounting for the disturbance of the water surface by introducing an effective gravitational acceleration parameter *g'* as shown by (Webber, 1991):

$$g' = g\frac{(\rho_w - \rho_l)}{\rho_w} \tag{47}$$

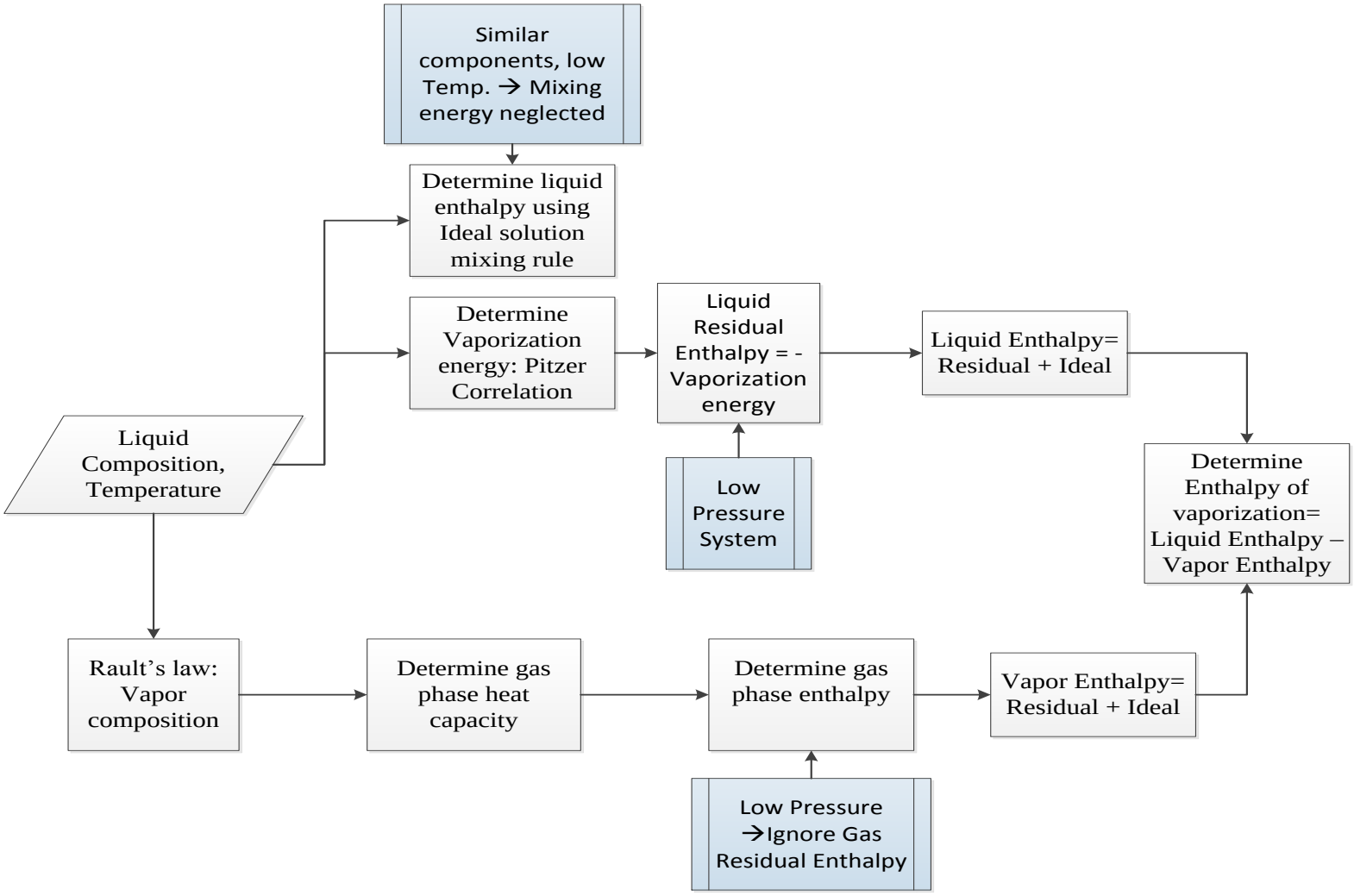

Figure 13: Algorithm for thermodynamic effects as implemented in the proposed model

CHAPTER VI

ANALYSIS OF GOVERNING PHENOMENA

6.1.Introduction

The pool spreading model developed in this work was used to identify the relative importance of the phenomena involved in the pool spreading process of a cryogenic liquid mixture like LNG. The purpose of this analysis was to gain a better perspective of the effect of these phenomena and how their effect varies throughout the lifetime of the spreading pool. This should provide a better idea so as to optimize the modeling processes and approaches required when conducting a sensitivity analysis.

A base case was defined before conducting the sensitivity analysis. The purpose of this Base Case was to be used as a reference simulation. The base case was compared to several simulations which included or not the phenomena involved in the pool spreading process of a cryogenic liquid mixture. The base case was selected so as to represent the most commonly used approaches in modeling the mechanical and heat effects involved in the pool spreading process. Mechanical effects were modeled using a gravity-inertia balance, whereas heat effects were modeled using an adjusted simple 1-D conduction.

The effect of the following phenomena was studied in this analysis:

1. Friction and gravity terms
2. Thermal contact/ roughness adjustment parameter

3. Boiling heat transfer
4. Mixture thermodynamics

6.2.Definition of the base case

The Base Case was defined as follows:

- The liquid spreading is LNG. The properties of the LNG mixture are shown in Table 10.
- LNG spreads on concrete. The physical properties for concrete were extracted from Briscoe & Shaw (1980) as shown in Table 11.
- The pool spreads according to a gravity inertia regime as represented by Webber (1991), as shown in Equation 19.
- 1-D conduction is used to represent heat transfer, as shown in equation 49.

$$\frac{dm}{dt} = \frac{Q}{\Delta H_{vap}} = \frac{\chi k (T_a - T_b)}{\Delta H_{vap} (\pi \alpha)^{0.5}} \int_0^{r(t)} \frac{2\pi r' dr'}{(t - t')^{0.5}} \tag{48}$$

The simulations were run for two scenarios:

- A 1000 m^3 instantaneous spill.
- A 10 m^3/s continuous spill for 100 seconds.

These scenarios have been adopted from Briscoe and Shaw (1980).

Table 10: LNG properties used in simulation

Density	450 kg/m^3
Molecular Weight	16.043 kg/kmol
Latent Heat of vaporization	8.8 kJ/mol
Composition	Methane: 89.9 %, Ethane: 6 %, Propane: 2.2 %, Butane: 1.5 %, Nitrogen: 0.4 %

Table 11: Concrete properties used in simulation

Density	2300 kg/m^3
Specific Heat	961.4 J/kg-K
Thermal Conductivity	0.92 W/m-K
Thermal Diffusivity	4.16×10^{-7} m^2/s

6.3.Friction and gravity terms

Frictional effects are an important parameter in the momentum balance implemented in many of the currently available models. Yet the applicability of implementing frictional effects for boiling liquids has been questioned (Brambilla *et al.,* 2009). Frictional effects of boiling cryogenics are usually corrected for by incorporating empirical constants to better predict the spreading behavior of LNG. These empirical constants are either based on experimental work developed for LNG as is the case with Briscoe & Shaw (1980), or based on mathematical derivations for the spread of boiling water as with

Webber (1991), which brings their validity and versatility for application into question. In this section, the relative importance of frictional effects on the gravitational driving force is investigated. This was done by comparing both terms of the gravity inertia regime as shown in Equation 49.

$$\frac{d^2r}{dt^2} = \underbrace{\frac{4g_r h}{r}}_{Gravity} \underbrace{-\beta\frac{(dr/dt)^2}{h}}_{Friction} \tag{49}$$

When compared to the gravitational driving force, the effect of friction is seen to be significant towards the later stages of the pool lifetime as shown in Figure 14 .

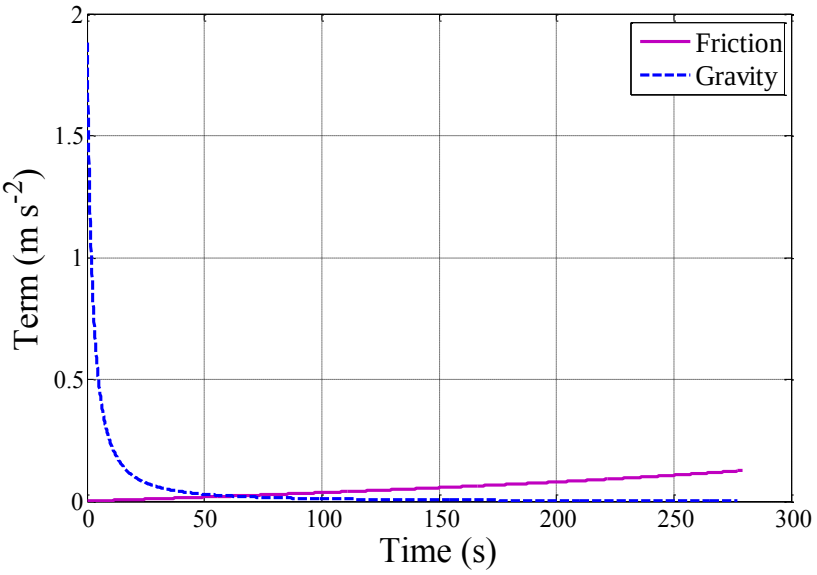

Figure 14: Webber 1991 model with 1-D ideal conduction: gravity and friction comparison

Therefore, when the momentum balance is coupled with 1-D conduction to model the pool behavior, frictional effects are expected to be significant towards the later stages of the pool lifetime.

Moreover, adding or removing the frictional term will affect the value of the gravitational driving force of the pool as shown in Figure 15. As expected, when friction is removed from the gravity inertia balance equation, the gravitational driving force increases throughout the pool lifetime.

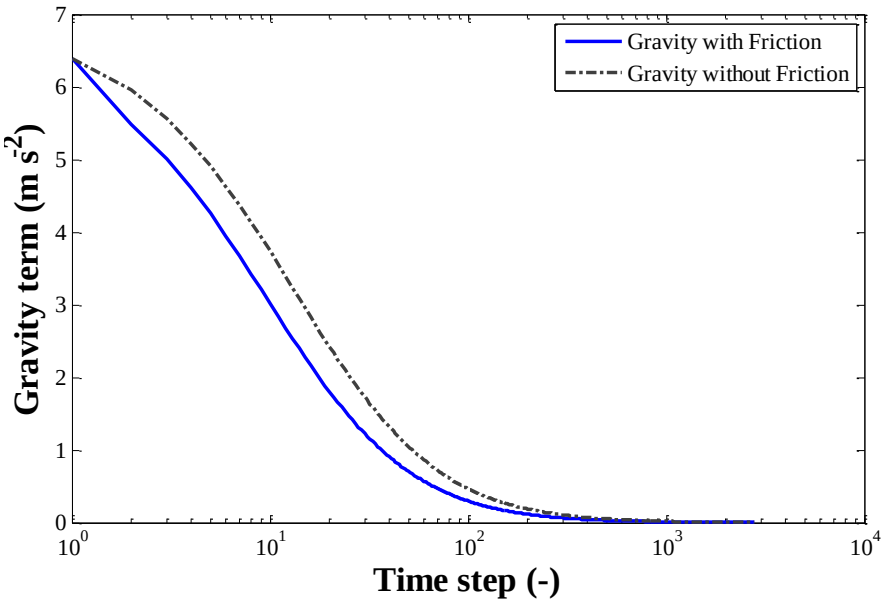

Figure 15: Effect of friction on gravitational driving force

Similarly when comparing the pool radius for both cases, the pool will spread faster when the friction term is removed, but will have a shorter lifespan due to the larger area

in thermal contact with the substrate as shown in Figure 16. Nonetheless, although these effects are not overly significant, the addition or removal of friction will completely change the pool's overall behavior, as the addition of friction will result in a smaller pool that lasts longer.

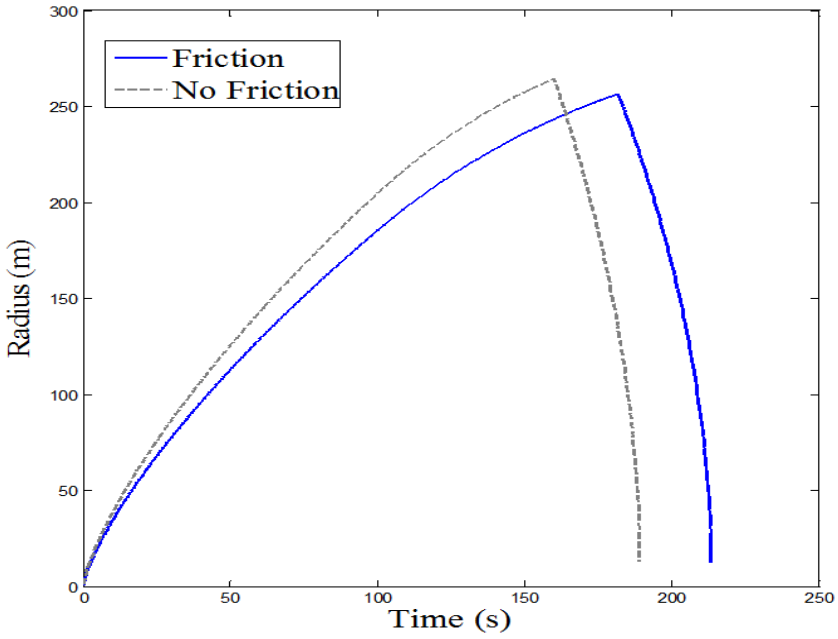

Figure 16: The effect of friction on pool radius

6.4.Effect of thermal contact/ roughness

When trying to model the boiling heat transfer observed with LNG using 1-D conduction, an empirical constant (χ) has been employed to adjust for perfect thermal contact as shown by Briscoe & Shaw (1980) (equation 49) and Jensen (1983) (Equation 4). A value of $\chi = 3$ has been commonly used based on laboratory scale experiments of

liquid Nitrogen on a galvanized Iron plate (Burgess & Zabetakis, 1962). The validity of this constant to applications involving different spill scenarios and different substrates has not been questioned. Therefore a sensitivity analysis was conducted to determine the effect of this parameter on the pool spread model, Figures 17 and 18 show the effect of varying this parameter for the two cases with and without friction.

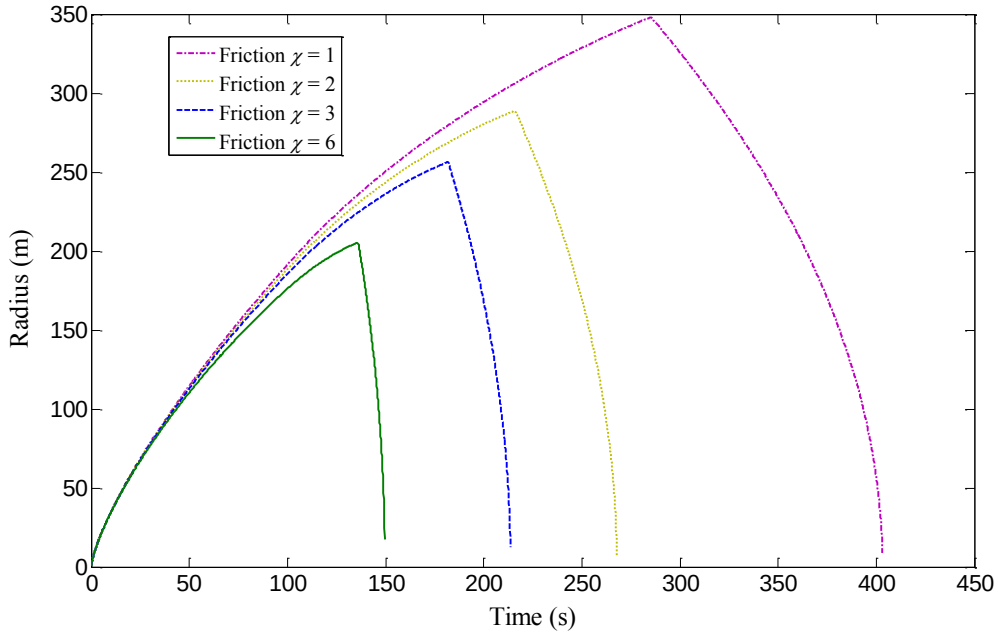

Figure 17: Effect of varying thermal contact parameter on pool radius while maintaining frictional effects (Base Case: χ=3)

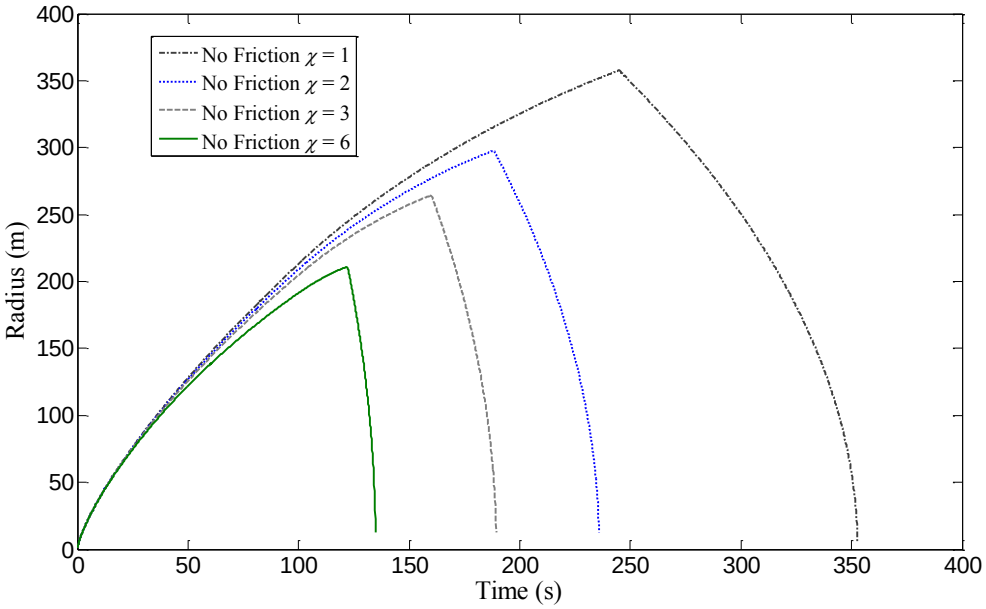

Figure 18: Effect of varying thermal contact parameter on pool radius while ignoring frictional effects (Base Case: χ=3)

The 1-D conduction model seems to be very sensitive to this parameter which implies that perhaps further investigation is required to determine its validity and applicability to LNG on different substrates. Better experimental data would be required to increase confidence in the applicability of these empirical parameters for LNG spill scenarios.

6.5.Heat transfer and boiling mechanism

In this section, the base case which assumes 1-D conduction (with χ = 3) was compared to the pool spread model incorporating the boiling correlations described in Section 2.1 above. Other effects such as mixture thermodynamics have not been repressed for the sake of this comparison to help capture the true effect of implementing different heat

transfer mechanisms. Figure 19 to 27 show the effect of implementing boiling heat transfer on the pool spread and heat flux for both a continuous and instantaneous spill. It is important to note that frictional effects were ignored when boiling heat transfer correlations are used since direct contact between the ground and the spreading pool is limited throughout the pool's lifetime by either a vapor film or bubbling; nonetheless they were included in the Base Case.

Due to the high initial superheat, the pool will initially be in the film boiling regime, but there are two possible mechanisms that can lead to a change of the boiling regime to nucleate boiling. First, the cooling of the substrate may reduce the temperature difference between the liquid and the substrate and promote film collapse. Second, preferential boiling of the lighter hydrocarbons, will increase the content of heavier components in the pool, which would destabilize the film (Conrado & Vesovic, 2000). It is important to recall that although mechanical effects could also promote film collapse and the transition between boiling regimes, these effects have not been considered as they have not been extensively studied in literature. Instead, film stability and transition between boiling regimes is governed solely by heat effects, primarily the temperature superheat difference between the substrate and the spreading LNG.

Implementing boiling correlations will results in higher values of the maximum pool radius and pool lifetime for both continuous and instantaneous spills, this is because heat transfer and subsequently the vaporization rate will be limited by film boiling. The

complexity of the boiling process of LNG on land or sea renders its complete description difficult. Thus the modeling of the boiling of an LNG mixture requires more theoretical and experimental efforts. Moreover, further work is needed to increase confidence in the validity of the correlations used to calculate the heat transfer for the different boiling regimes and the values of ΔT_{CHF} or ΔT_{min} in the case of an LNG mixture.

For a continuous spill, implementing boiling heat transfer will result in a 50 m difference in estimating the maximum pool radius, this difference is maintained throughout the pool decay period. Although the difference in pool diameter is not significant during the pool development period and 1-D conduction provides a reasonably close estimate using a much simpler correlation, the difference becomes important towards the end of the pool lifetime, as implementing boiling mechanisms will predict a pool that lasts longer by about 60s or 125% longer than that predicted using 1-D conduction. Properly estimating the pool lifetime from the source term will have an important effect on predicting subsequent effects, particularly in the case of the formation of a vapor cloud.

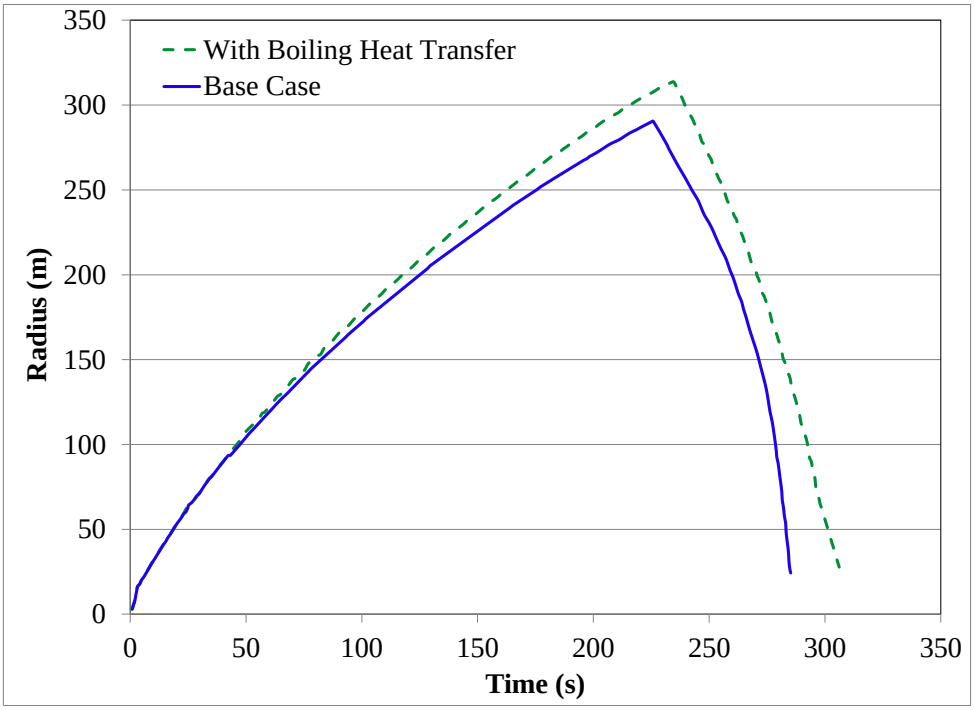

Figure 19: Effect of boiling heat transfer on pool radius for a continuous spill

Moreover, when comparing the heat flux curves as shown in Figures 20 and 22, there is an initial order of magnitude in difference between the two models during the very early stages of pool contact, this difference decreases with time, but heat flux from 1-D conduction remains higher throughout the pool lifetime. In this scenario, the pool will remain in film boiling due to its relatively short lifetime. Additionally when comparing the ground temperature profiles as shown in Figure 21, implementing the boiling heat transfer mechanism will provide a more accurate representation of how the ground temperature changes, in contrast to 1-D conduction which is limited by its use of a Drichilet boundary condition to estimate the ground temperature.

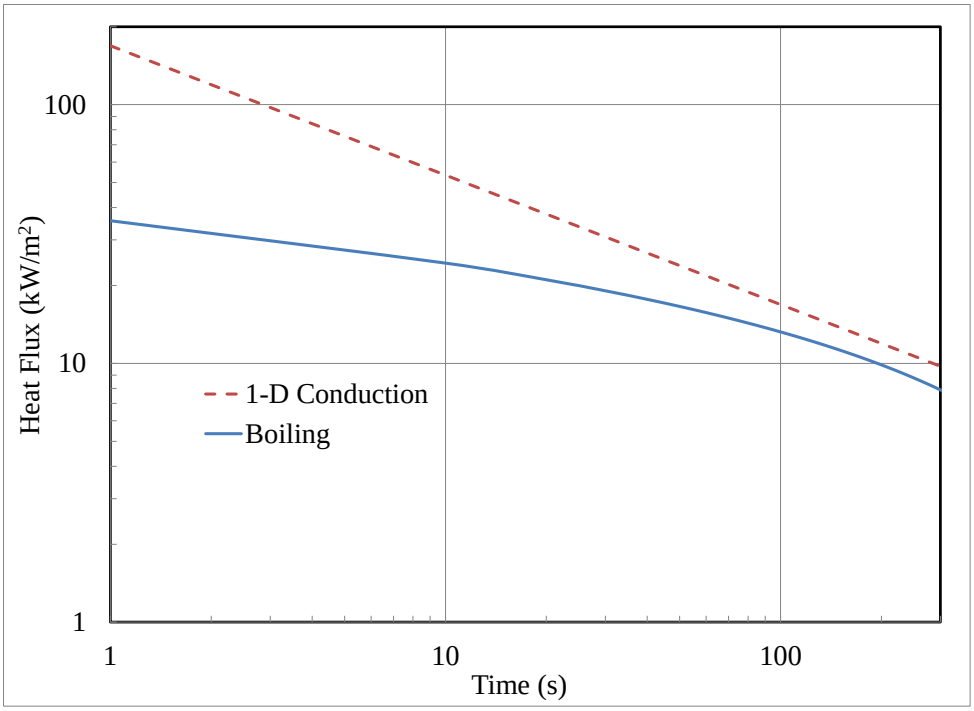

Figure 20: Effect of boiling heat transfer on heat flux at center of the pool for a continuous spill

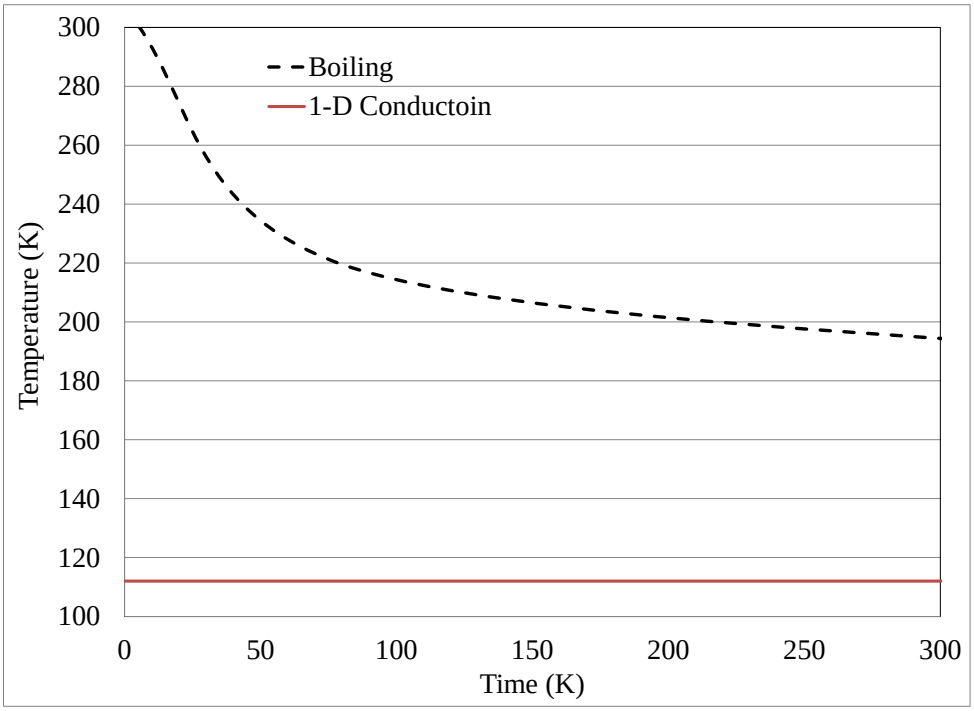

Figure 21: Effect of boiling heat transfer on temperature at center of the pool for a continuous spill

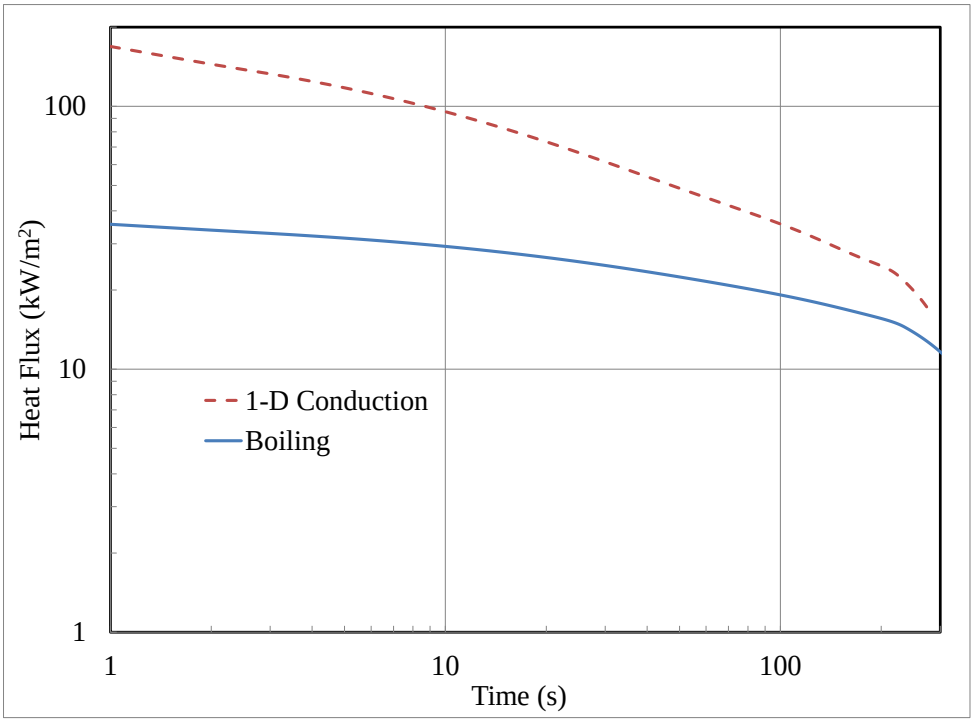

Figure 22: Effect of boiling on overall heat flux into pool for a continuous spill

Similarly in the case of an instantaneous spill, similar effects are observed when comparing the two heat transfer mechanisms; boiling effects are very similar to 1-D conduction when during the pool development stage but start to become important during the later stages of the pool lifetime, additionally implementing boiling effects will result in a longer pool lifetime. The main observed difference is observed when comparing the heat transfer flux curves. When comparing the heat flux at the center of the pool, boiling effects will predict a change in the boiling regime after 347 s of contact. The move from film to transition boiling is clearly observed with a spike in the heat flux value, nonetheless, this phenomena is very short lived and does not have a significant effect on the overall behavior of the heat flux curve. The effect of changing boiling

regimes becomes more significant when considering the larger picture as shown in Figure 26 which shows the overall heat flux of the pool instead of the local effect at the center of the pool shown in Figure 24. In this case the multiple spikes towards the end of the curve shows how different areas of the pool will reach the transition boiling regimes at different times due to varying contact times as the pool is spreading. Moreover, when comparing the temperature profiles, the point of film breakup and switch to transitional boiling regime is clearly observed and represented by a sudden drop in temperature as the liquid is now in direct contact with the ground instead of having an insulating vapor layer between them.

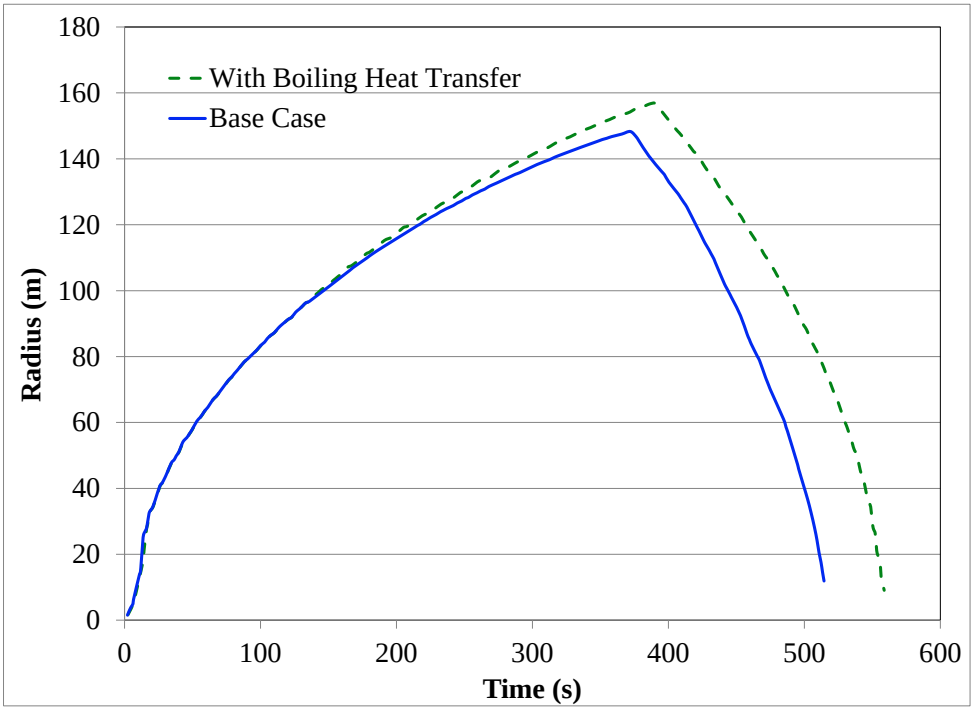

Figure 23: Effect of boiling heat transfer on pool radius for an instantaneous spill

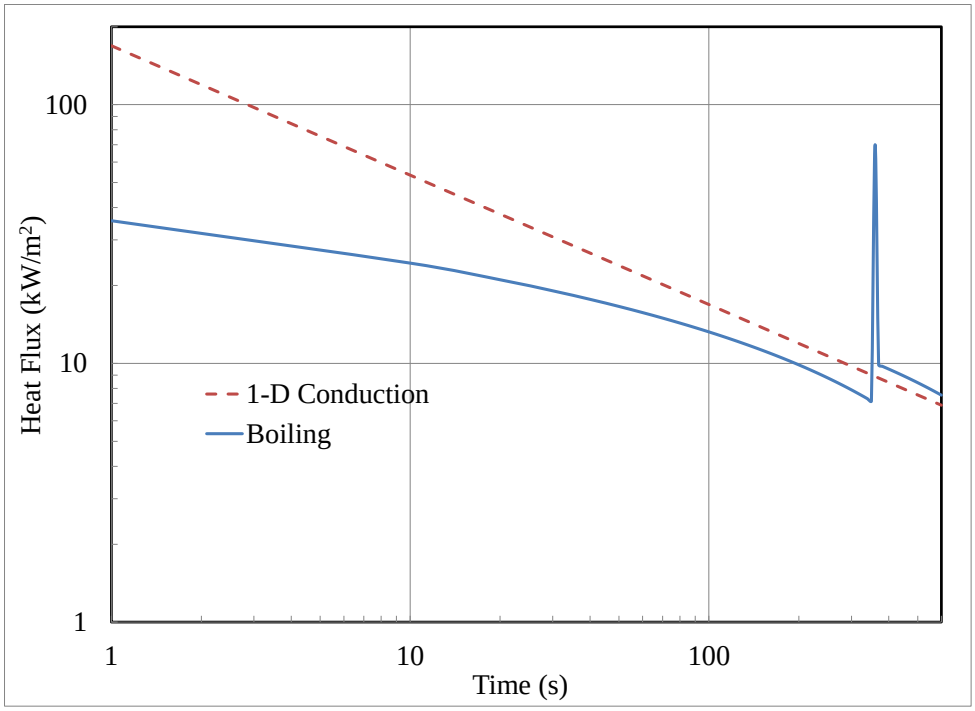

Figure 24: Effect of boiling heat transfer on heat flux at center of the pool for an instantaneous spill

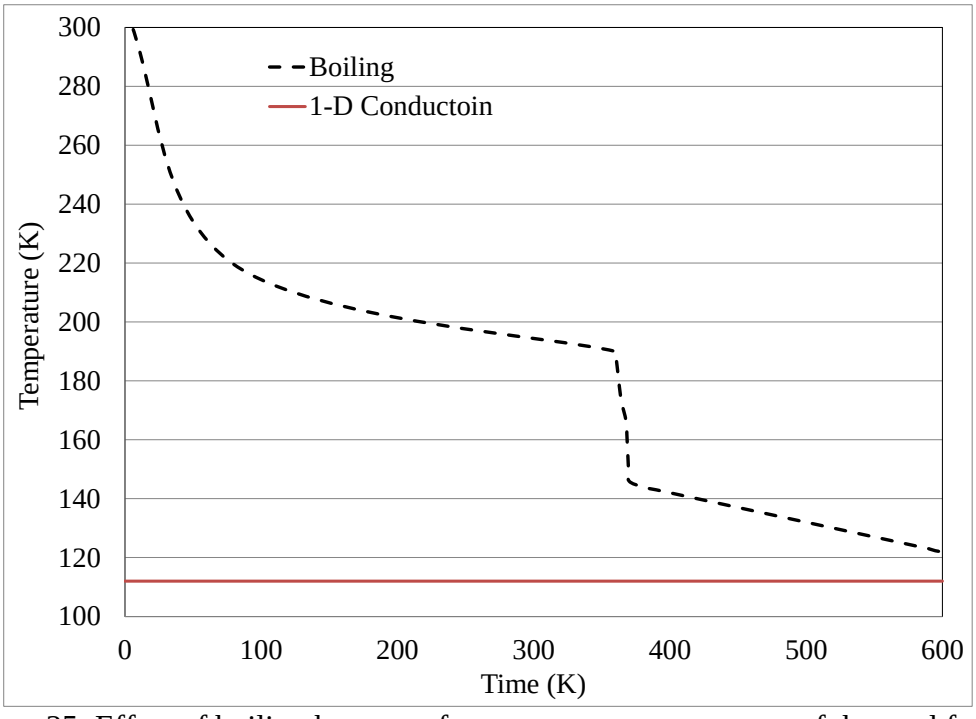

Figure 25: Effect of boiling heat transfer on temperature at center of the pool for an Instantaneous spill

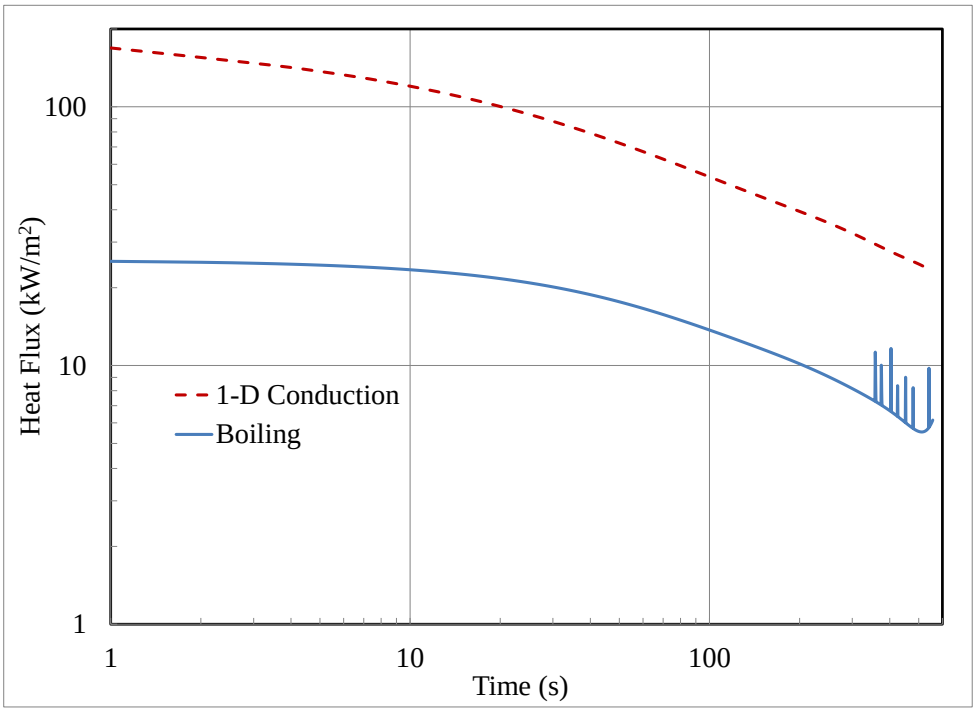

Figure 26: Effect of boiling on overall heat flux into pool for a continuous spill

Although representing heat transfer effects using boiling heat transfer correlations compared to adjusted 1-D conduction does not provide a significant difference, it offers a more accurate representation of the spill scenario and provides a better understanding of the dynamics of the ground-liquid heat transfer interaction. When comparing the effects of varying the χ parameter on 1-D conduction to boiling heat transfer as shown in Figure 27, it is clear that the commonly implemented adjusted 1-D conduction with χ=3 provides a reasonable representation of the pool behavior. Nonetheless, it is important to realize that the boiling heat transfer correlations are based on pure thermo physical properties of the spilled substance and the substrate and do not employ any empirical adjustment parameters such as the χ parameter used in 1-D conduction. Although boiling

heat transfer correlations will, as is the case with any thermo physical model, employ empirical parameters at the very basic levels, these parameters have not been implemented to adjust the nature of these predictions as is the case with the χ parameter. This difference in the nature of the boiling heat transfer correlations provides better confidence in their applicability to a wider range of spill scenarios on different substrates or even involving different cryogens.

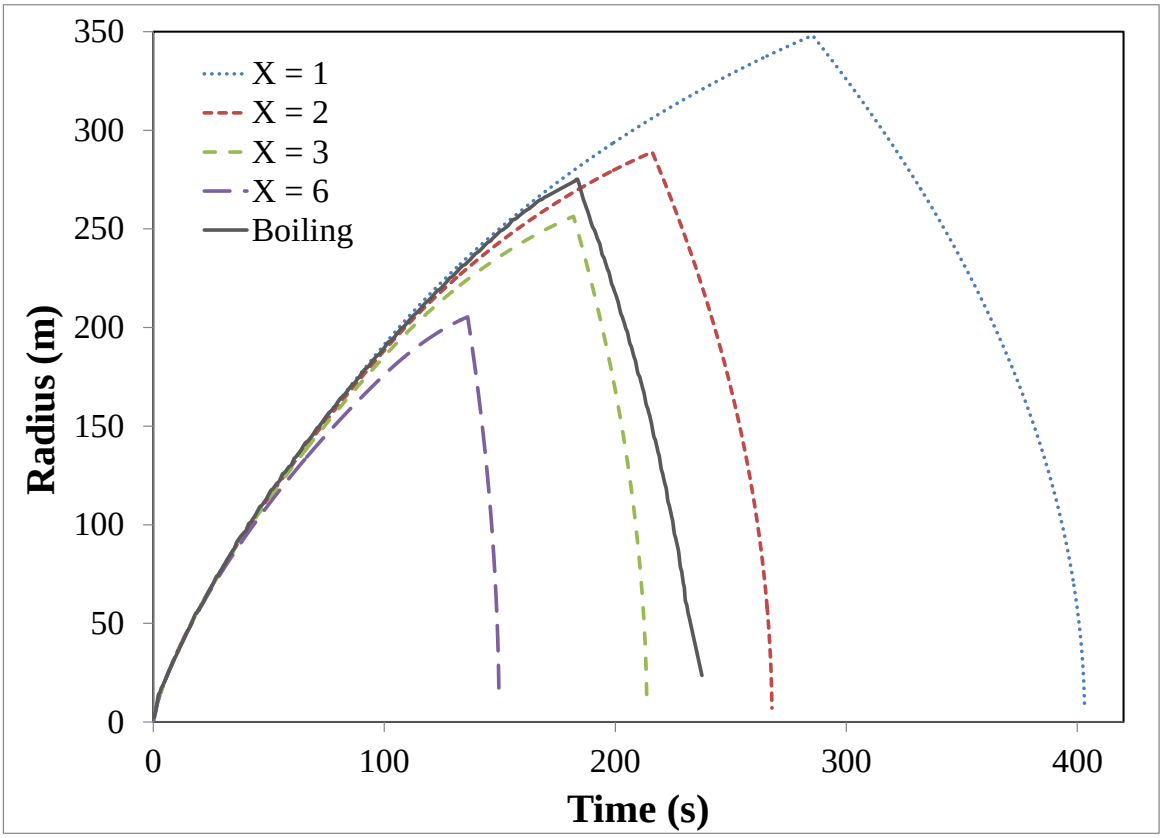

Figure 27: Comparing 1-D conduction with varying χ parameter to boiling heat transfer

6.6. Vapor liquid equilibrium (VLE) effects

Here, the base case was compared to the model incorporating VLE effects. VLE and mixture thermodynamics were implemented as described in Section 2.2.4 to determine the temperature, thermo physical properties and vapor and liquid compositions throughout the pool's lifetime. The initial composition of the LNG mixture used is shown in Table 1. In this comparison, heat transfer effects were modeled using 1-D conduction to obtain an absolute effect of mixture thermodynamics on the pool spreading process.

As shown by Figure 28 incorporating mixture and thermodynamic effects will not result in a significant enhancement to the pool spread model for continuous spills. This is primarily due to the continuous supply of fresh LNG into the pool which will maintain a high methane content as shown in Figure 29, yet once the continuous spill stops at 100s and the effect of preferential boil-off starts being more significant, the pool density and latent heat will start to increase due to the higher fractions of heavier hydrocarbons in the pool as shown in Figure 30 and 31. This in turn will affect the pool radius and the deviation of pool radius from 1-D conduction can be observed to begin after 100s which is the end time of the continuous spill as shown in Figure 28.

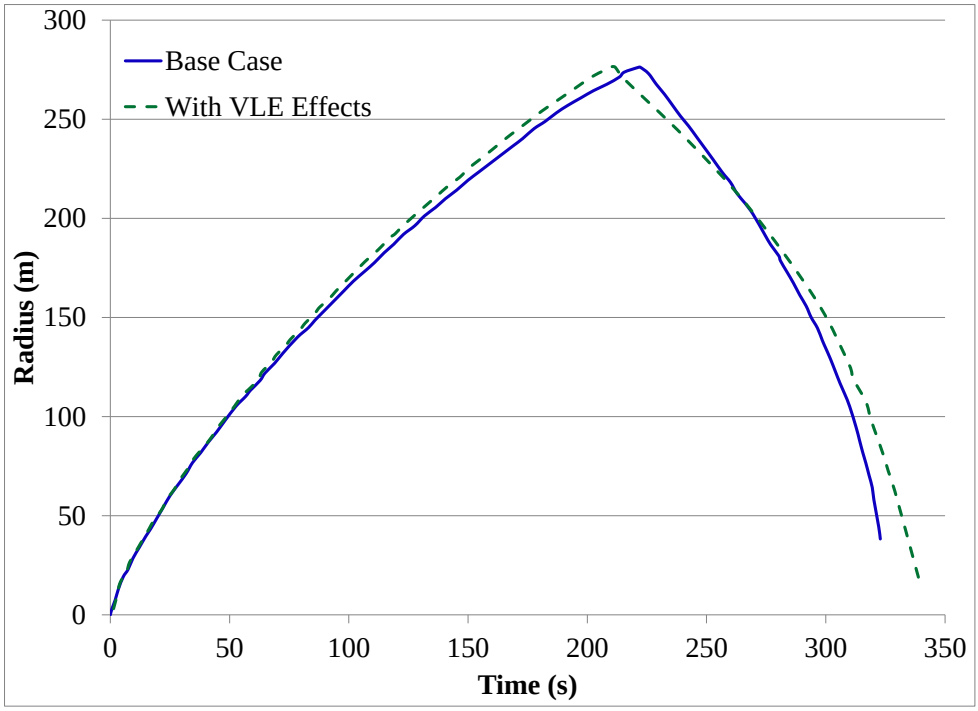

Figure 28: Effect of incorporating VLE effects on pool radius for a continuous spill

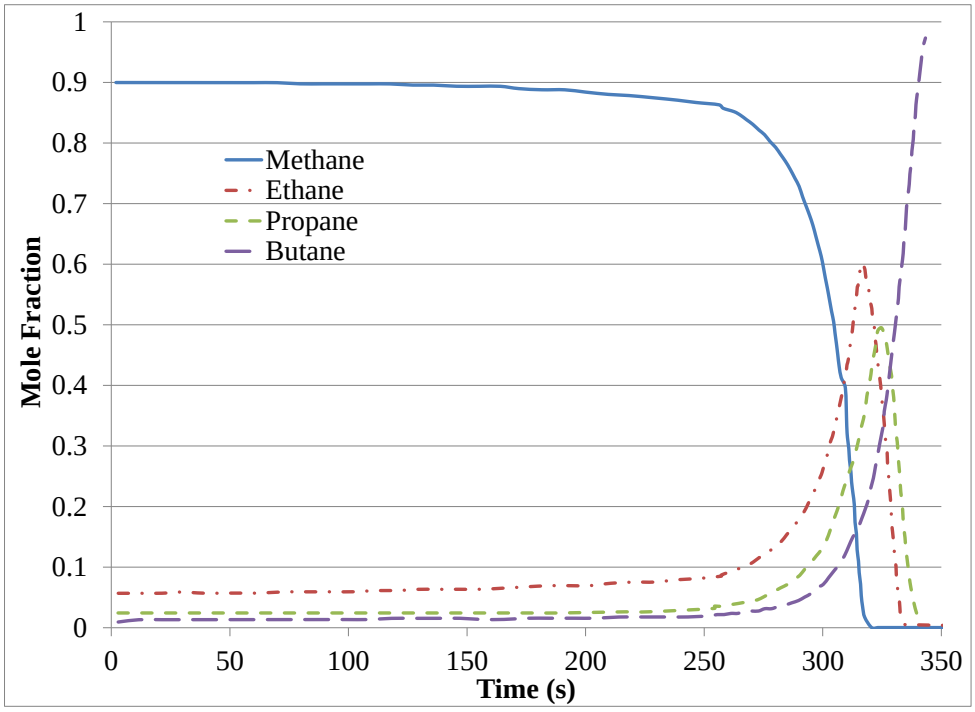

Figure 29: Effect of incorporating VLE effects on pool composition for a continuous spill

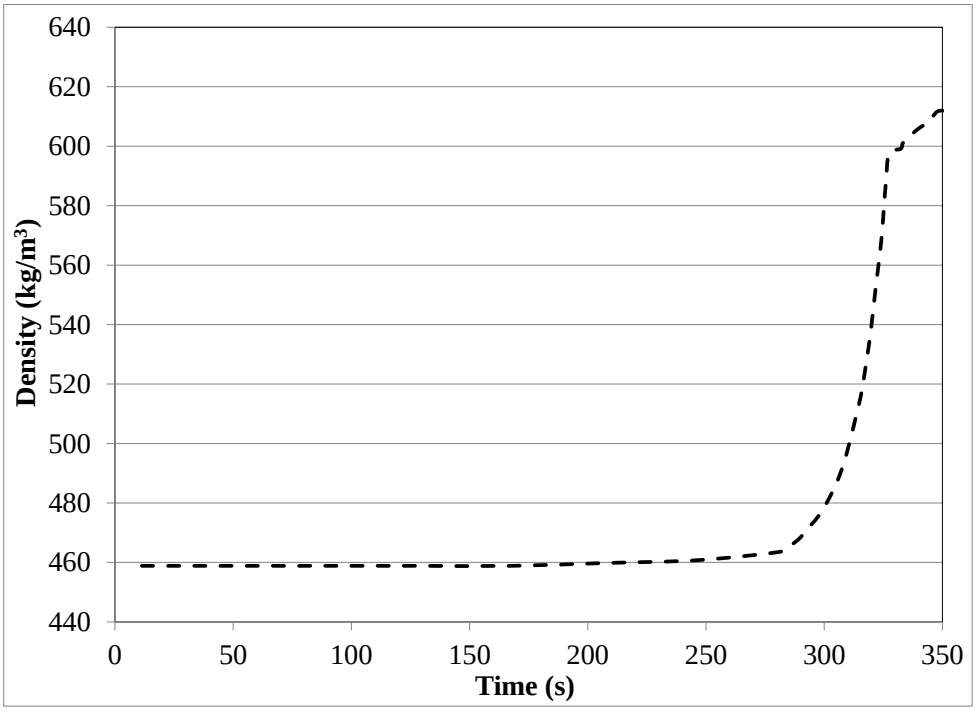

Figure 30: Effect of incorporating VLE effects on pool density for a continuous spill

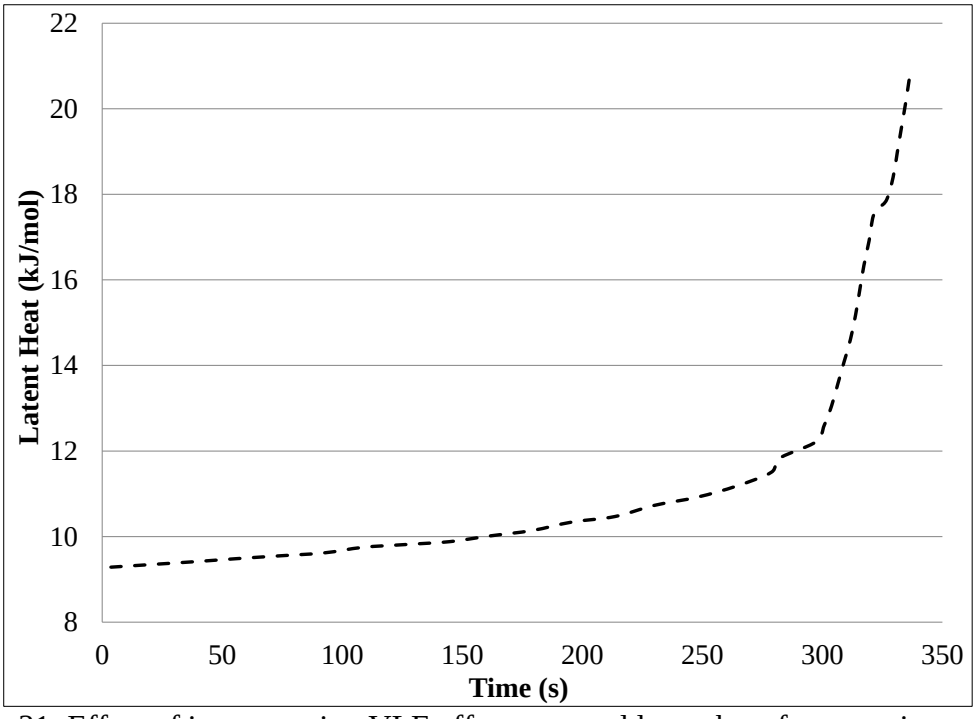

Figure 31: Effect of incorporating VLE effects on pool latent heat for a continuous spill

Similarly, for instantaneous spills, VLE effects are significant only for the pool decay period. Implementing VLE will predict a longer pool lifetime by about 80s or about 120% longer than using a simple LNG analogue as shown in Figure 32. This is primarily due to the immediate effect of preferential boil off on the pool's composition and thermo physical properties as shown in Figures 33to 35 since there is no continuous supply or replenishment of the lighter methane as is the case with a continuous spill. The effect of incorporating VLE on the pool radius is parallel to the change in the pool composition due to preferential boiling. Similarly, the density and the latent heat will increase as the fraction of heavier hydrocarbons starts increasing in the pool.

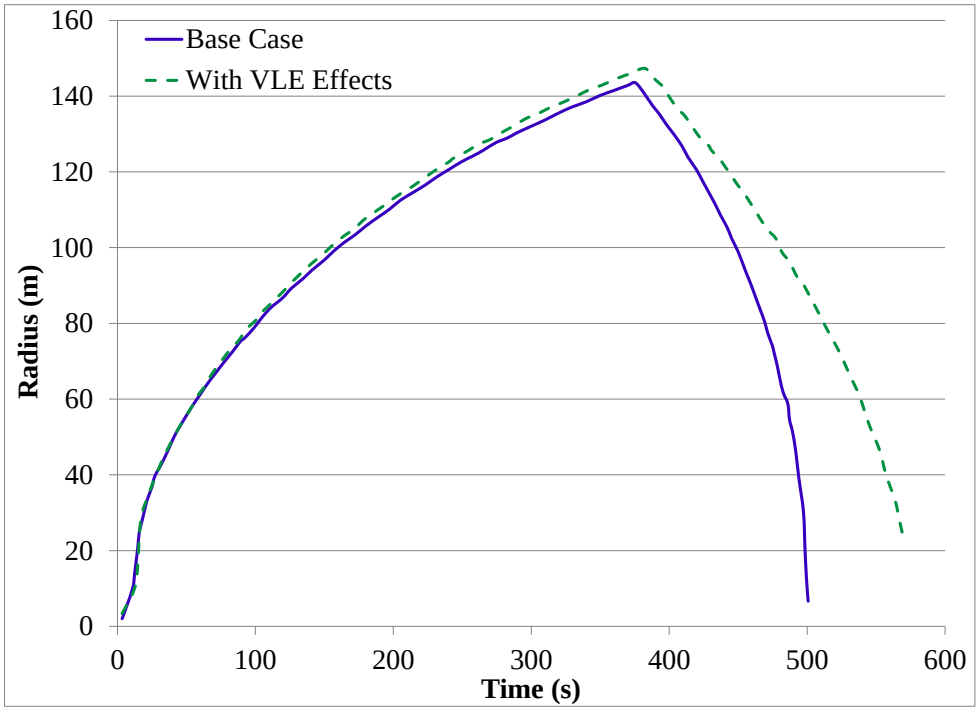

Figure 32: Effect of incorporating VLE effects on pool radius for an Instantaneous spill

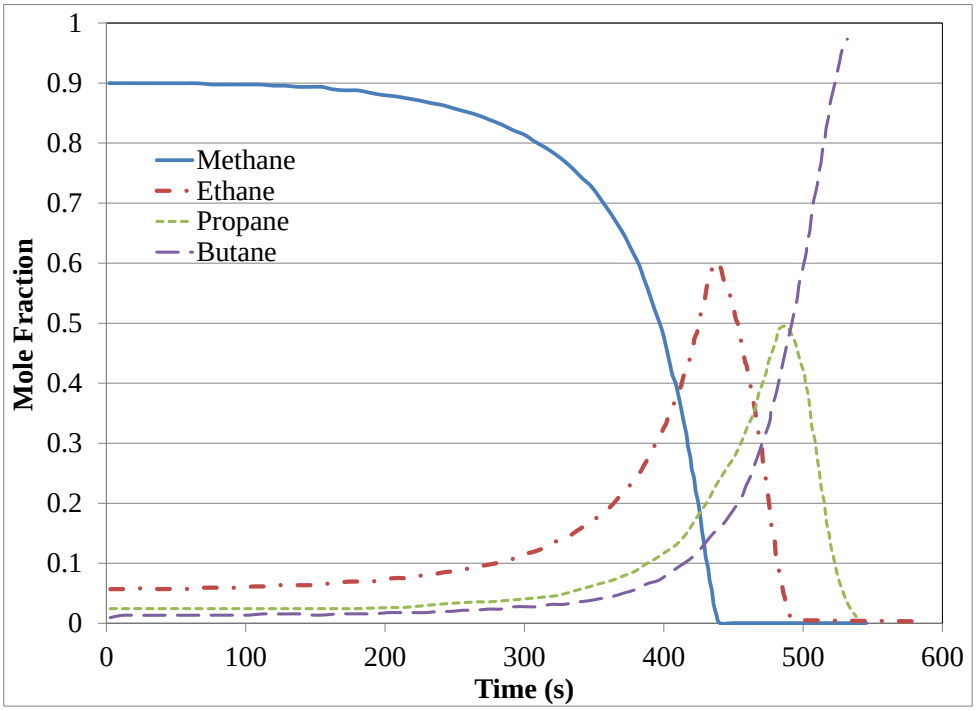

Figure 33: Effect of incorporating VLE effects on pool composition for an Instantaneous spill

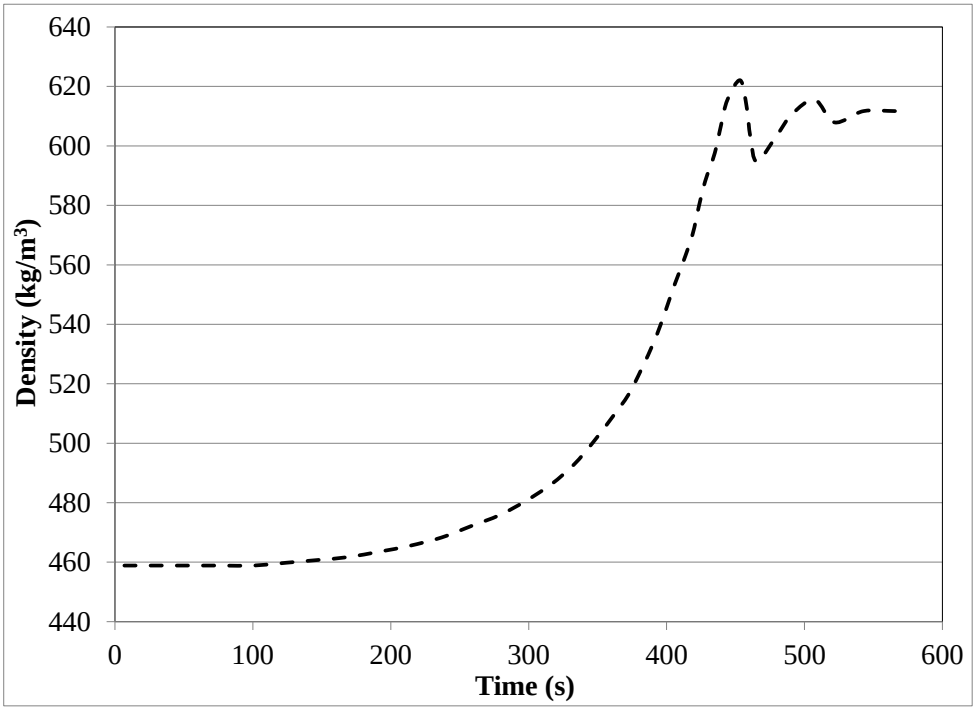

Figure 34: Effect of incorporating VLE effects on pool density for an Instantaneous spill

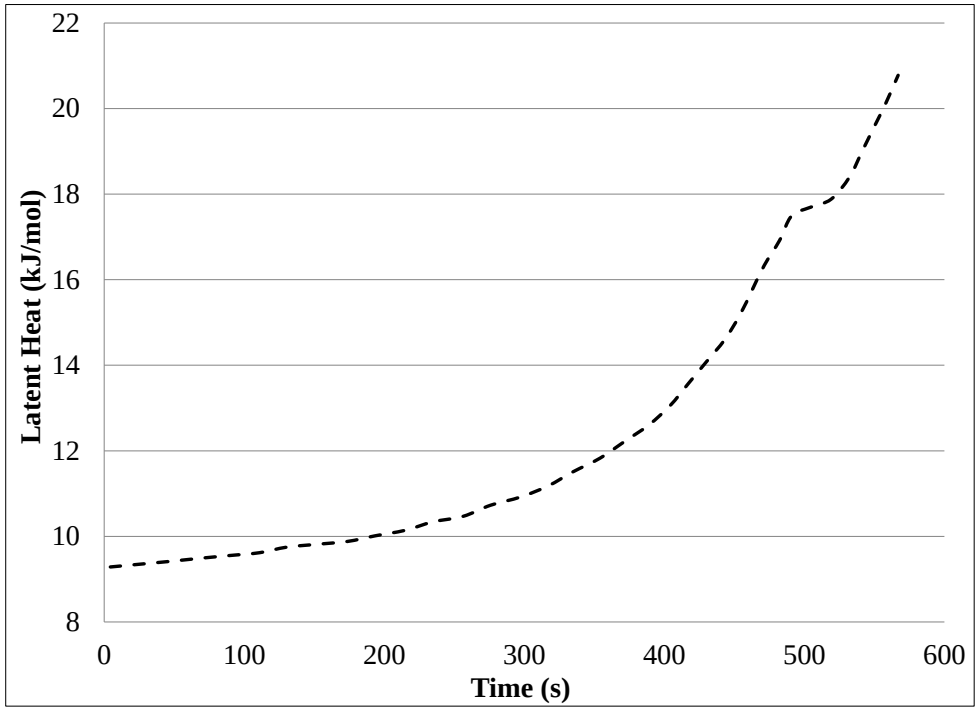

Figure 35: Effect of incorporating VLE effects on pool latent heat for an Instantaneous spill

Although, the overall effect of implementing VLE is not very significant it offers a multitude of thermo physical properties throughout the pool lifetime and provides a unique perspective on the pool's dynamics throughout its lifetime. This is a reasonable and important enhancement to available models since it increases the understanding of the underlying behaviors and phenomena without exerting a huge computational load.

6.7.Conclusion of sensitivity analysis

The following conclusions can be drawn from this sensitivity analysis:

1. 1-D conduction models were found to be very sensitive to the thermal contact correction parameterχ, which brings into question the versatility of applying 1-D conduction to represent heat transfer under different scenarios. Further experimental work is required if adjusted 1-D conduction is to be used with LNG.

2. Frictional effects within the Base Case seem to have a noticeable effect on the pool spreading process and become important during the later stages of the pool spread. However, this is not applicable in the case of LNG, as its unique nature as a cryogen, prevents the use of conventional frictional terms which may simply overestimate the friction as stated by (Brambilla *et al.,* 2009). In this model, the use of boiling heat transfer correlations while ignoring frictional effects seem to be in reasonable agreement with the Base Case that employs adjustable parameters to correct for frictional and heat effects.

3. The model which includes the boiling effects provided results close to the current 1-D conduction model with a correction factor χ=3. .It provides a better representation of the pool boiling behavior, the ground temperature change and the transitions between the different boiling regimes during the pool spreading.

4. VLE and mixture effects seem to have a negligible effect on the pool spreading process during methane rich periods of the pool's lifetime, but become increasingly significant during the methane poor periods as the effect of preferential boiling becomes more observed. Additionally, implementing VLE effects will provide a detailed insight on the varying thermo physical properties throughout the pool's lifetime.

CHAPTER VII

MODEL VALIDATION

7.1.Introduction

When trying to validate the model for spills on land and sea, there are very few well instrumented data for medium and large scale experiments in literature. Such lack of data presents some limitations when used to validate the complex phenomena involved in the pool spreading process. More experimental investigations at significantly larger scales on land and sea are necessary to properly validate the existing LNG pool spreading models. Nonetheless, two sets of data for land and sea were selected from the literature and compared to the full present model incorporating mixture thermodynamics, VLE effects and varying boiling heat transfer regimes was validated.

7.2.Validation for spills on land

Moorehouse and Carpenter (1982) conducted a series of experiments on soil and concrete involving continuous releases of LNG at a rate of 17 tonnes/hr on soil and 14 tonnes/hr on concrete. The model was compared to a set of experiments conducted on concrete with thermal conductivity and diffusivity of 1.7 W/m-K and $5x10^{-7}$ m^2/s. As shown by Figures 36 and 37, the model is able to reproduce the data reasonably well. Nonetheless it is important to consider that the measured data is only for the pool development stage of the release and is therefore governed primarily by momentum effects, and may not be used to properly validate the modelling of heat effects into the spreading pool.

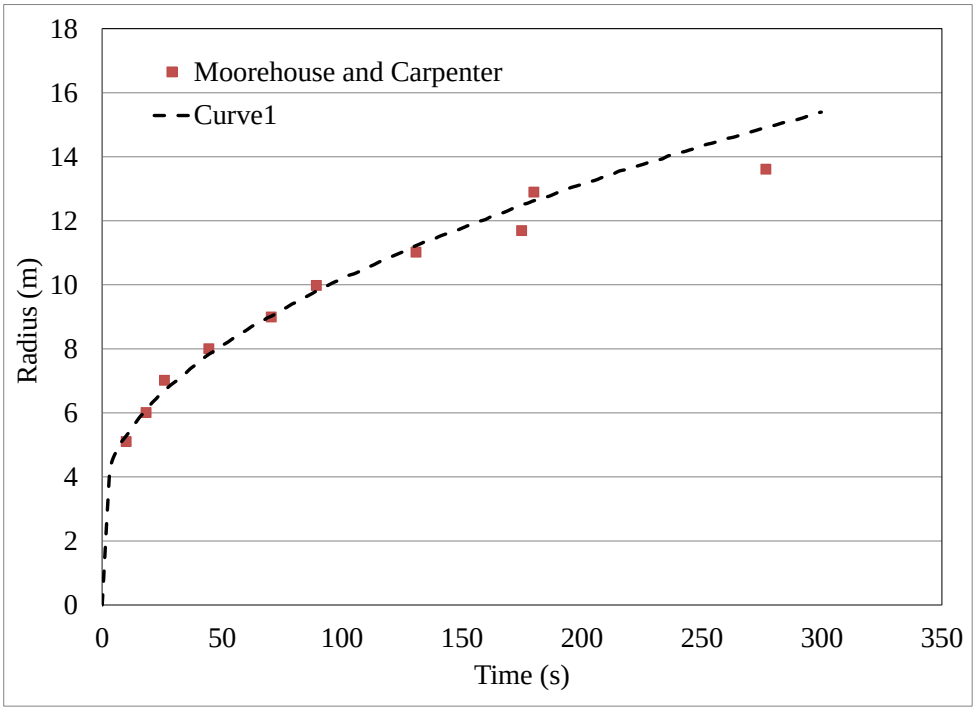

Figure 36: Model validation vs experimental data for a 17 tonne/hr continuous LNG release on concrete

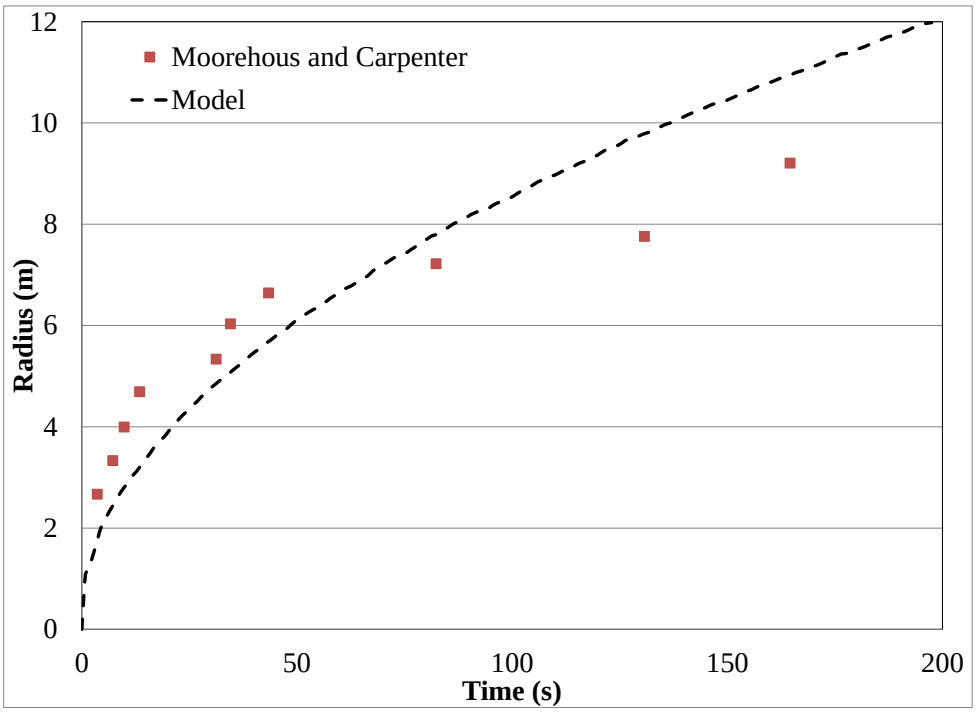

Figure 37: Model validation vs experimental data for a 14 tonne/hr continuous LNG release on soil

7.3.Validation for spills on sea

The Esso 11 experiments included a continuous release of 0.15 m^3/s of LNG on sea, the experimental data was extracted from Hissong (2007). As shown in Figure 38 the model seems to validate reasonably well with the experimental data, yet the validation suffers from the same uncertainty as that on land as the experimental data only measures the very early stages of pool development. Moreover the availability of only four experimental points weakens the credibility of the data to be used for validation purposes.

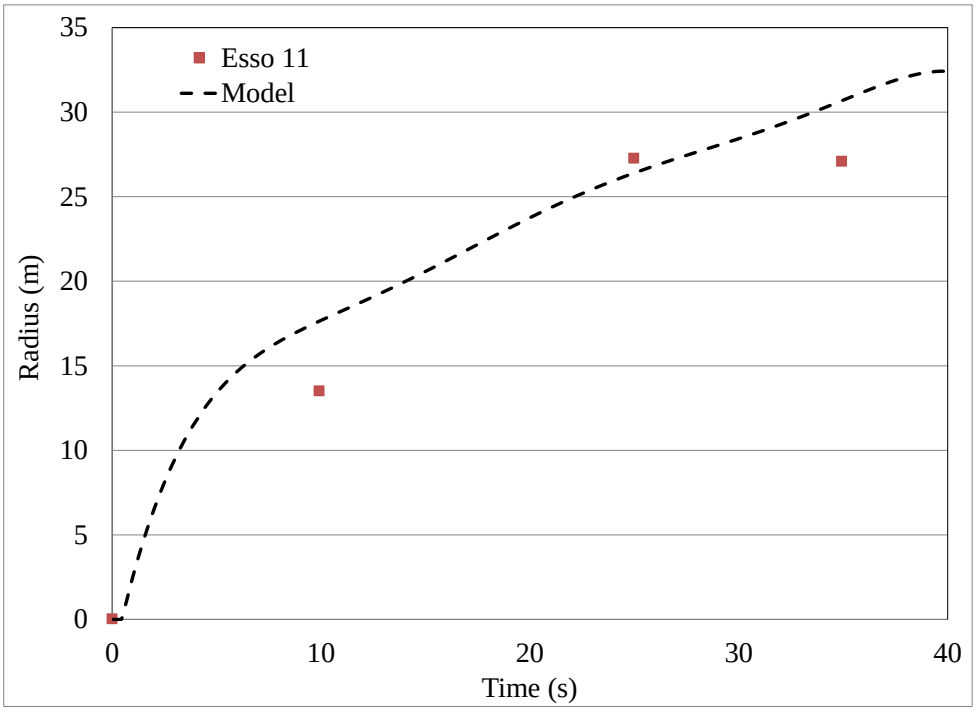

Figure 38: Model validation vs experimental data for a continuous release of 0.15 m3/s of LNG on sea

CHAPTER VIII

CONCLUSION

In this work, a pool spread model was developed by incorporating boiling heat transfer and mixture thermodynamic effects to a gravity inertia momentum balance. The aim was to develop an analytical model that represents the unique properties of LNG as accurately as possible without relying on any empirical or adjustment parameters.

A sensitivity analysis was conducted to determine the relative importance of boiling heat transfer, friction, thermal contact/roughness adjustment parameter and VLE effects on the rate of pool spreading and decay. The purpose of the sensitivity analysis was to determine the effect of increasing the complexity of the currently available models and to analyse the sensitivity of these models to the empirical constants incorporated.

Modelling conduction using boiling heat transfer rather than 1-D conduction seems to have a significant effect on pool spreading, particularly towards the later stages of the pool spread as these effects start to become increasingly significant. On the other hand, implementing VLE and mixture effects into the model seems to have a negligible effect when compared to using fixed LNG thermo physical properties for continuous spills, but are significant for instantaneous spills. This is due to delayed effect of preferential boil off in continuous spills due to the continuous supply of fresh LNG into the pool, unlike

the case for an instantaneous spill where the effect of preferential boil off occurs much quicker.

The addition of friction to the gravity inertia balance was investigated to better understand its relative importance on the mechanical aspects of the pool spread model, this is because frictional effects have been ignored in the developed model due to the implementation of boiling heat transfer which assumes that the leading edge of the pool will always be in film boiling and therefore sliding on a thin frictionless vapour film.

Results show that friction seems to have a noticeable effect on the pool spreading process modelled using the Base Case, and will affect the pool lifetime and spread rate, particularly towards the later stages of the pool lifetime. This is explained by the fact that as the modelled pool spreads faster due to lack of friction, it will get thinner at a faster rate and will be in contact with more ground which increases the amount of heat conducted into the pool. These two effects will results in a pool with a shorter lifetime and a larger maximum diameter. However, this is not applicable then dealing with LNG due to its cryogenic nature, and the use of conventional frictional terms as will in fact over estimate these frictional effects as shown by (Brambilla *et al.*, 2009).

Finally, the effect of the thermal contact/roughness correction parameter was studied. The thermal contact/roughness correction parameter is an empirical parameter that has usually been introduced to early spread models such as Briscoe & Shaw (1980) and

Jensen (1983) to correct the 1-D conduction to match experimental data for LNG. When varied, the 1-D conduction equation was found to be very sensitive to this parameter which brings into question its applicability to a wide range of spreading scenarios and substrates.

The model was validated against experimental data found in literature. The model seems to validate well with the available data, but since all of the data found was only for the development region of the pool this brings into question the confidence they provide in validating this model. A more reliable set of experimental data are required to properly validate and understand the governing phenomena involved in pool spread models.

CHAPTER IX

FUTURE WORK

Further work is needed to understand substrate effects on the boiling behaviour of LNG. The effect of surface roughness, porosity, thermal conductivity and other parameters on the boiling process needs to be studied to properly determine their effect on bubble nucleation and film breakup. Additionally, CFD modelling of these phenomena may be required to provide additional insight on the effect of these parameters. Nonetheless, the author of this report strongly believes that experimental work, both lab and large scale, is crucial to gain a better understanding and develop more accurate correlations when dealing with LNG. Although modelling efforts are important, there has been a lack of experimentally backed insight during recent years, particularly when it comes to dealing with the boiling phenomena of LNG. Experimental work at medium and large scale is currently being planned to be conducted at the Ras Laffan Emergency and Safety College, which could be a huge step forward to help properly and comprehensively validate the model and provide a better understanding of its governing phenomena.

REFERENCES

ABSG, & FERC. (2004). Consequence assessment methods for incidents involving releases from liquefied natural gas carriers.

Berenson, P. J. (1962). Experiments on pool-boiling heat transfer. *International Journal of Heat and Mass Transfer*, *5*, 985–999.

Boe, R. (1998). Void fraction measurements in boiling cryogenic mixtures using gamma densitometer. *International Journal of Heat and Mass Transfer*, *41*(10), 1167–1175.

Brambilla, S., & Manca, D. (2009). Accidents involving liquids: A step ahead in modeling pool spreading, evaporation and burning. *Journal of Hazardous Materials*, *161*(2-3), 1265–1280. doi:10.1016/j.jhazmat.2008.04.109

Briscoe, F., & Shaw, P. (1980). Spread and Evaporation of Liquid. *Progress in Energy and Combustion Science*, *6*(2), 127–140.

Burgess, D., & Zabetakis, M. G. (1962). Fire and explosion hazards associated with liquefied natural gas (p. 34). Washington, DC: U.S. Dept. of the Interior, Bureau of Mines, Report 6099.

Cavanaugh, T. A., Siegell, J. H., & Steinberg, K. W. (1994). Simulation of Vapor Emissions From Liquid Spills. *Journal of Hazardous Materials*, *38*(1), 41–63. doi:10.1016/0304-3894(93)E0111-E

Conrado, C., & Vesovic, V. (2000). The influence of chemical composition on vaporisation of LNG and LPG on unconfined water surfaces. *Chemical Engineering Science*, *55*(20), 4549–4562. doi:10.1016/S0009-2509(00)00110-X

Drake, E. M., Jeje, A. A., & Reid, R. C. (1975). Transient boiling of liquefied cryogens on a water surface: I. Nitrogen, Methane and Ethane. *International Journal of Heat and Mass Transfer*, *18*(12), 1361–1368. Retrieved from http://www.sciencedirect.com/science/article/pii/0017931075902495

Fay, J. A. (1971). Physical processes in the spread of oil on a watersurface. *Proceedings of The Joint Conference on Prevention and Control of Oil Spills* (p. 463467).

Fay, J. A. (2007). Spread of large LNG pools on the sea. *Journal of Hazardous Materials*, *140*(3), 541–551. doi:10.1016/j.jhazmat.2006.10.024

Forsman, B. (2011). *North European LNG Infrastructure Project : A Feasibility Study for an LNG filling station infrastructure and test of recommendations* (p. 20).

Hansen, O., Melheim, J., & Storvik, I. (2007). CFD-modeling of LNG dispersion experiments. *AIChE Spring National Meeting, 2007*, (April). Retrieved from http://www.gexconus.com/doc/olav/LPS_Houston_Hansen_2007.pdf

Hissong, D. W. (2007). Keys to modeling LNG spills on water. *Journal of Hazardous Materials*, *140*(3), 465–477. doi:10.1016/j.jhazmat.2006.10.040

Hoult, D. (1972). Oil spreading on the sea. *Annual Review of Fluid Mechanics*, *341*(1). Retrieved from http://www.annualreviews.org/doi/pdf/10.1146/annurev.fl.04.010172.002013

Jensen, N. O. (1983). On cryogenic liquid pool evaporation. *Journal of Hazardous Materials*, *8*(2), 157–163. doi:10.1016/0304-3894(83)80054-5

Kalinin, E. K., Berlin, I. I., Kostyuk, V. V., & Nosova, E. M. (1976). Heat transfer in transition boiling of cryogenic liquids. *Advances in Cryogenic Engineering*, *21*, 273–277.

Klimenko, V. V. (1981). Film boiling on a horizontal plate — new correlation. *International Journal of Heat and Mass Transfer*, *24*(1), 69–79. doi:10.1016/0017-9310(81)90094-6

Liu, Y., Olewski, T., Vechot, L., Gao, X., & Mannan, S. (2011). Modelling of a cryogenic liquid pool boiling using CFD code. *14th Annual Symposium, Mary Kay O'Connor Process Safety Center "Beyond Regulatory Compliance: Making Safety Second Nature"* (pp. 512–524).

Luketa-Hanlin, A. (2006). A review of large-scale LNG spills: Experiments and modeling. *Journal of Hazardous Materials*, *132*(2-3), 119–140. doi:10.1016/j.jhazmat.2005.10.008

Moorhouse, J., & Carpenter, R. J. (1986). Factors affecting vapour evolution rates from liquefied gas spills. *North western Branch Papers, Institution of Chemical Engineers*, *1*, 4.1–18.

NFPA 59A Standard for the Production, Storage, and Handling of Liquefied Natural Gas (LNG) (2009).

Opschoor, G. (1975). *Investigations into the spreading and evaporation of burning LNG-spills on water and the heat radiation from LNG-fires on water* (No. CTI-TNO 75-03777, I.O.W.-subproject 4, report 4). Apeldoorn.

Opschoor, G. (1980). Spreading and evaporatoin of LNG spills and burning LNG spills on water. *Journal of Hazardous Materials, 3*(3), 249–266. doi:10.1016/0304-3894(80)85004-7

Puttock, J. S., Blackmore, D. R., & Colenbrander, G. W. (1982). Field experiments on dense gas dispersion. *Journal of Hazardous Materials, 6*,13–41.

Raj, and A.S. Kalelkar, (1974) "Assessment Models in Support of the Hazard Assessment Handbook", U.S. Coast Guard Report No. CG-446-3, Report submitted by Arthur D. Little, Inc., to Department of Transportation, U.S. Coast Guard, Contract No. DOT-CG24655A, January 1974.

Raj, P. K. (1981). Models for cryogenic liquid spill behavior on land and water. *Journal of Hazardous Materials, 5*(1-2), 111–130. doi:10.1016/0304-3894(81)85009-1

Reid, R. C., & Wang, R. (1978). The boiling rates of LNG on typical dike floor materials. *Cryogenics, 18*(7), 401–404. doi:http://dx.doi.org/10.1016/0011-2275(78)90033-4

Webber, D. M. (1987). "Heat conduction under a spreading pool", UKAEA Report SRD/HSE R 421.

Webber, D. M. (1991). Source terms. *Journal of Loss Prevention in the Process Industries, 4*(1), 5–15. doi:10.1016/0950-4230(91)80002-C

Webber, D. M. (1996). Letter to the editor. *Journal of Hazardous Materials, 45*(1), 79–80. doi:10.1016/0304-3894(95)00043-7

Webber, D. M. (2012). On models of spreading pools. *Journal of Loss Prevention in the Process Industries, 25*, 923–926.

Woodward, J. L., & Pitblado, R. (2012). *LNG Risk Based Safety - Modeling and Consequence Analysis* (p. 374). Wiley-AIChE.